Accepted Manuscript

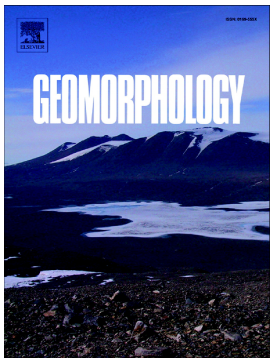

Rise and fall of a small ice-dammed lake - Role of deglaciation processes and morphology

Nehyba Slavomír, Hanáček Martin, Engel Zbyněk, Stachoň Zdeněk

PII: S0169-555X(17)30043-0
DOI: doi: 10.1016/j.geomorph.2017.08.019
Reference: GEOMOR 6114

To appear in: *Geomorphology*

Received date: 10 January 2017
Revised date: 17 July 2017
Accepted date: 6 August 2017

Please cite this article as: Nehyba Slavomír, Hanáček Martin, Engel Zbyněk, Stachoň Zdeněk , Rise and fall of a small ice-dammed lake - Role of deglaciation processes and morphology, *Geomorphology* (2017), doi: 10.1016/j.geomorph.2017.08.019

This is a PDF file of an unedited manuscript that has been accepted for publication. As a service to our customers we are providing this early version of the manuscript. The manuscript will undergo copyediting, typesetting, and review of the resulting proof before it is published in its final form. Please note that during the production process errors may be discovered which could affect the content, and all legal disclaimers that apply to the journal pertain.

ACCEPTED MANUSCRIPT

Rise and fall of a small ice-dammed lake - role of deglaciation processes and morphology

Nehyba Slavomír[1], Hanáček Martin[1,2], Engel Zbyněk[3], Stachoň Zdeněk[4]

[1]Department of Geological Sciences, Faculty of Science, Masaryk University, Kotlářská 2, 611 37 Brno, Czech Republic; slavek@sci.muni.cz, HanacekM@seznam.cz

[2]Centre for Polar Ecology, Faculty of Science, University of South Bohemia in České Budějovice, Na Zlaté stoce 3, 370 05 České Budějovice

[3] Department of Physical Geography and Geoecology, Faculty of Science, Charles University in Prague, 128 43 Praha, Czech Republic; engel@natur.cuni.cz

[4]Department of Geography, Faculty of Science, Masaryk University, Kotlářská 2, 611 37 Brno, Czech Republic; zstachon@gmail.com

Abstract

A small ice-dammed lake, which developed along the margin of Nordenskiöldbreen on the northern coast of Adolfbukta, (central Spitsbergen, Svalbard) has been studied by a combination of facies analysis, ground penetrating radar, analysis of photos and satellite imagery, and by surface mapping by Unmanned Aerial Vehicle (drone). The lake existed between the years 1990–2012 and occupied two partial depressions in the bedrock, separated by a bedrock ridge for the dominant period of its history. Whereas the eastern depression was almost completely infilled due to direct fluvial input, the western depression revealed only thin sedimentary cover and was dotted from the eastern depression by an outflow of surficial waters. Gilbert delta deposits with typical tripartite zones of topset, foreset and bottomset were recognised

ACCEPTED MANUSCRIPT

in the eastern depression. Topset was comprised by deposits of a braided river. Foreset is formed by deposits of sediment gravity flows (turbidity currents and debris flows). Bottomset is represented by alternating suspension deposits and deposits of hyperpycnal underflows (low-density turbidity currents). The ruling factors of the evolution of the delta were glacier retreat, bedrock morphology, both affecting the relative lake level, and the rate of sediment delivery. Glacier retreat over stepped and inclined bedrock morphology led to delta prograding and downstepping. The recognised fluvio-deltaic terraces revealed four lake level falls followed by fluvial downcutting, erosion and redeposition of the older deltaic/lake deposits, the shifting of the lake´s position towards the damming glacier and the transition of the sediment input in the same direction. The termination of the lake was a result of further glacier retreat and the opening of subglacial drainage.

Keywords: Svalbard, Nordenskiöldbreen, Gilbert delta, stacking pattern, glacier dam retreat, basin floor morphology, fluvio-deltaic terraces.

1. Introduction

Landscape and environmental changes of the glacial realm are commonly well recorded in the deposits of glacial lakes. Special attention has been devoted to the deposits of ice-dammed lakes because of catastrophic floods (Knight, 2003; Russel, 2007, 2009), effects of meltwater release on subglacial (Shaw, 2002) and proglacial environments (Magilligan et al., 2002), or spectacular ice-dam failures (Teller, 1995; Fischer et al., 2002). The presence and drainage of subglacial and proglacial lakes also have wider implications for terrestrial ice sheet stability, and marine processes including thermohaline circulation (Clark et al., 2001; Teller et al., 2002).

ACCEPTED MANUSCRIPT

Ice-dammed lakes develop during both ice-sheet advance and retreat; however, they are typically connected with the ice-sheet decay (Donnelly and Harris, 1989; Johnsen and Brennand, 2006; Winseman et al., 2004). Recent deglaciation processes in the polar realm give rise to the formation of such lakes. Small and closed lake basins are commonly characterized by rapid lake-level fluctuations. In this paper, we will document the sedimentary history of a small ice-dammed lake (78°40.44'N, 16°54.48'E) that existed from 1990 to 2012 at Nordenskiöldbreen (Svalbard). The lake was filled by a coarse-grained Gilbert delta complex, with the feeding stream sediment delivery oriented constantly towards the damming glacier. The first brief and rather general information about the existence of the study deposits was provided by Stacke et al. (2013).

Deltaic successions play an important role in the sedimentary infill of ice-dammed lakes (Clemmensen and Nielsen, 1981; Martini, 1990; Aitken, 1995). Alluvial deltas are complex depositional systems and their stratigraphy is often used to infer changes in the water level, the energy of the basin and the sediment supply (Giosan and Bhattacharya, 2005). The studied case is an excellent field example of a delta system, controlled by rapid base-level changes, glacier retreat and bedrock morphology (the role of subsidence, compaction, waves or tides is neglected) and so should be included in the sequence stratigraphic interpretation of complex glacigenic sedimentary environments, which are still undervalued compared with most other sedimentary environments.

2. The study area and locality

Nordenskiöldbreen glacier represents one of several joined ice tongues which descend into Adolfbukta (Fig. 1). The middle part of the glacier calved into the sea

ACCEPTED MANUSCRIPT

bay after the climax of the Little Ice Age (LIA) (Rachlewicz et al. 2007). Nordenskiöldbreen is classified as a tidewater outlet glacier with a polythermal regime (Evans et al., 2012; Hambrey and Glasser, 2012; Ewertowski et al., 2016; Rachlewicz et al., 2007). The lateral margins of the glacier terminate in the terrestrial realm, on the northern and southern coast of Adolfbukta (Fig.1). Nordenskiöldbreen glacier retreated rapidly from the end of the 19th century until the 1960s of the 20th century. Glacier retreat significantly decreased since then, which is explained by the shallowing of the bay in the front of the glacier snout (Rachlewicz et al., 2007). Zones of both the basal debris-rich ice and the upper clean coarse crystal ice can be observed along the vertical walls of the Nordenskiöldbreen; the zone of the basal debris-rich ice is up to 2.5 m thick and the total glacier thickness along its north-western margin is about 10 m.

The LIA-proglacial zone is located on the hillside of the mountain ridge and declines towards Nordenskiöldbreen glacier and the coast of the bay along the northern side of the Adolfbukta. Outcrops of metamorphic rock dominate in the proximal part of the proglacial zone due to significant dynamics of the relief. The bedrock is predominantly formed by Precambrian mica schists, marbles and amphibolites (Dallamann et al., 2004). Thin and discontinuous sediments cover the basement here, which was reshaped into rouches moutonnées with polished and scratched surfaces. The proglacial zone is poured through by streams of meltout water. These streams are incised into the basement; their directions are governed by the basement structures (Fig. 1, 2). Channels are relatively straight; the braiding style is only local. Some streams are oriented towards the glacier due to the basement tilt (generally between 2^{o} and 5^{o}).

ACCEPTED MANUSCRIPT

The studied area is located on the margin of Nordenskiöldbreen on the northern coast of Adolfbukta (Figs. 1, 2). Large glacially abraded elevations of basement here are broken up by significant fractures, along which tight and relatively deep gorges were formed. The gorges are perpendicular to the north-eastern margin of the glacier. Two of these gorges, separated by a rock ridge (Fig. 2), played a crucial role in the formation of the studied lake. The eastern depression is narrow and prolonged in the NNW-SSE direction. The western depression is more open and less elongate in the NW-SE direction. The glacier terminates both depressions on the surface on their E-SSE sides (Fig. 2). The barrier of the glacier is oriented in the NNE-SSW direction. Evidence that the lake occupied both depressions is given by preserved deposits and image data. Draining of the lake and subsequent vertical fluvial incision led to outcropping of several meters thick deposits in the eastern depression. A meltwater stream cut the sedimentary succession into the crystalline bedrock. The eastern depression is almost filled with deposits and morphologically distinct terraces have been recognised on the surface (Figs. 2, 3). The western depression contains only a thin sedimentary blanket.

3. Methods of study

The evolution of the lake and deltaic system can be reconstructed for the time period 1990–2012 and is based on the results of satellite images and photos of the glacier, facies analysis and ground penetrating radar scanning.

3.1. Satellite imagery

The study of the evolution and properties of the ice dammed lakes was maintained by aerial photographs taken in 1961 and 1990 and from 2009 QuickBird imagery, photos of the glacier front for the years 2000, 2001, 2005, 2008, 2009, 2012

ACCEPTED MANUSCRIPT

and 2013 and from http:// toposvalbard.npolar.no. These remote sensing data were supplemented in July 2015 by images obtained from an unmanned aerial vehicle (UAV). A UAV (hexacopter type) equipped with a GoPro HD Hero 3+ Black edition (flight level 50 m above ground, described in detail in Stuchlík et al., 2016) was used for orthophoto imaging and digital elevation model (DEM) generation. Ground control points were captured by using a GNSS (Global Navigation Satellite System) receiver (Trimble Geoexplorer Geo XH 6000 series). The positions captured were postprocessed using base station data. These data also provide information about surficial deposits and associated landforms, especially fluvio-deltaic terraces at different levels.

3.2. Facies analyses

Lithofacies analysis, according to Tucker (1988), Walker and James (1992) and Nemec (2005), is based on sedimentary structures and textures. Several artificial sections have been cut by the Authors into the steep walls of the eastern depression and logged (position of the artificial outcrops is presented in Fig. 2.

3.3. Ground penetrating radar (GPR) scanning

GPR data were collected along two longitudinal profiles on fluvio-deltaic terraces in the eastern depression (Figs. 2, 3). The first profile was undertaken in terrace II and the second was carried out from terrace III to terrace IV. GPR profiling was carried out using a shielded 250 MHz antenna and RAMAC CU-II control unit (MALÅ GeoScience, 2005). The signal acquisition time was set to 188 ns and scan spacing to 0.05 m. The GPS receiver and the UAV-based DEM were used to determine coordinates and elevation for the corresponding traces. GPR data were processed using REFLEXW software, version 7.0 (Sandmeier, 2012). The raw GPR profiles were filtered using a subtract-mean (dewow) and background removal.

ACCEPTED MANUSCRIPT

Finally, the radargrams were corrected for topography (static correction) using the DEM-derived elevation data. The depth axis of profiles was converted from the time axis using a wave velocity of 0.11 m ns^{-1}. The velocity was determined from the bedrock depth measured in the exposed vertical sections and from the position of the relevant reflector in obtained GPR scans. The velocity of 0.11 m ns^{-1} falls within the range of values between 0.09 and 0.12 m ns^{-1} reported for in braided-river deposits and delta facies (Huggenberger, 1993; Heinz, Aigner, 2003).

.

4. Results

4.1. Lake evolution after satellite images and photographs

The evolution of the lake started about the year 1990, when both the eastern and the western bedrock depressions were still covered by glacier ice (Fig. 4a). A stream ran along the glacier margin and formed small bodies of stagnant water above local depressions of bedrock. One such stagnant water body was ice-dammed close to the NW edge of the eastern depression (Fig. 4a) and water probably intruded below the glacier. The disrupted glacier margin started to break and gain an arch shape with vertical margin walls. Such margins are visible in photos from the year 2000 (Fig. 4a). The lake gradually enlarged towards the SE, following the retreating snout of the glacier (Fig. 4a).

The change in direction of the feeding stream of the lake happened during the time period between 1990 and 2000 (Figs. 4a,b). The shift of stream trajectory towards SE observed is connected with gradual enlargement of the eastern depression in the same direction. The bedrock gorge entering this depression was at a higher inclination of the than was the dip of the former gorge where the stream channel had been located (gorge oriented towards SW) (Fig. 4b). The supporting

ACCEPTED MANUSCRIPT

stream entered directly into the eastern depression and progradation of the Gilbert delta started with formation of fluvio-deltaic terraces.

The formation of the small pond in the western depression is connected with the years 2000-2001 (compare Figs. 4a,b). This pond was separated from the rest of the lake because of a large, arched, NNW-SSE oriented bedrock ridge. The western depression did not have its own direct fluvial feeder and was subsidized by both water and sediment from the eastern depression for the whole time-span of the lake´s existence. The lake was continuously drained through the bedrock gorges towards the E - SE. Continued glacier retreat led to a further shift of the lake position and extent towards the SE (Figs. 4c, d).

The lake in the year 2009 is well documented by satellite image (toposvalbard.npolar.no). The eastern and the western depressions here communicate through lows of the bedrock ridge. The areal extent of the eastern depression was 14 382 m^2; however, the lake itself covered 3466 m^2. The western depression covered 11 029 m^2, and the extent of the lake here was 10 678 m^2. The Fig. 5 shows calving of the glacier into the lake and the draining of the lake in western depression through bedrock gorges.

The existence of the lake terminated after the year 2009 (Fig. 4e). Field data show that the lake did not exist in July 2012. The ice-dam was disrupted due to intense surficial and basal melting. These processes, together with an extended decay of the shelf ice in Adolfbukta, led to a weakening of glacier integrity and a subglacial burst of the ice-dam. The stream adjusted to the new profile, cutting deeply into the former deltaic deposits and reached the bedrock. The stream recently continues under the glacier. Eroded material was redeposited into the margins of Adolfbukta, where a new glaciomarine coarse-grained delta is being formed (Fig. 6).

ACCEPTED MANUSCRIPT

4.2. Terrace morphostratigraphy

A system of four (I-IV) fluvio-deltaic terraces has been documented by surface mapping (Fig. 3). The highest (altitude 42.7-42.2 m) terrace (terrace I) is located most distal to the glacier, as oldest terrace in the system. Lower terraces are located at successive positions down valley, closer to the damming glacier. The altitude of terrace II is 40.1-39.7 m, that of terrace III is 37.8 m and altitude of the lowest terrace (IV) is 36.6-36.2 m. Significant parts of the terrace sediments have been removed by fluvial incision and erosion, which are slowly destroying the sedimentary record of the lake.

Terraces are located along the right bank of the recent meltwater stream. However, they are not preserved at all levels to an equal extent and have only small extent along the left stream bank (mostly the lowest terrace IV) (Figs. 2,3). The surfaces of the terraces are nearly flat and they are inclined towards S – SSE with the angle of the dip between 1^{o} and 6^{o}. The terrace I reveal the relative highest angle of the surface dip. Only few traces of minor channels or small bars have been recognised on the terrace surfaces (similarly Eilertsen et al., 2011). These relatively shallow and flat channels cut are connected with recent torrential streams and were formed mostly after lake termination.

Terrace I was formed about the year 2000 (Figs. 7a,b). Terrace II was constructed by the year 2001 (Fig. 7b). A significant part of terrace IV was already built in the year 2005 (Figs. 7c,d), and by the year 2009 the terrace extent seems to reach its maximum. Terrace III must be therefore formed between the years 2001 and 2005. Lake terminated after the year 2009 (Figs. 6e).

ACCEPTED MANUSCRIPT

4.3. Facies analysis

The facies analysis of the sediments in artificial outcrops led to discrimination of fourteen lithofacies. Their characteristics and brief interpretations are presented in Table 1. Lithofacies have been grouped into four facies associations corresponding to four different depositional environments. Three of these environments correspond to tripartite (Gilbert-type) delta zones: topset (FA1), foreset (FA2) and bottomset (FA3) filling a proglacial lake. The downstream fining pattern can be followed (role of gravelly vs sandy lithofacies, mean grain size) from the uppermost FA1 to the lowermost FA3. The remaining FA 4 represents reworked subglacial material. The distribution and examples of both lithofacies and facies associations within the logged section is shown in Figs 8, 9, 10, 11 and 12. A typical subglacial environment with diamictites has not been recognised in the studied sedimentary sections; however, they might be preserved in peripheral parts of the studied area, which were not logged.

4.3.1. FA 1 - Delta topset - braided river deposits

These coarse-grained gravelly deposits have been recognised in all logged sections and represent 26.4% of relative thickness of deltaic deposits. They typically form the upper-most parts of the successions, form tabular to broadly lenticular bodies stacked vertically and laterally. The total thickness of FA 1 varies between 60 and 145 cm (average 99 cm). FA 1 is composed of three lithofacies (Gs, Gm and Gp - see Fig. 10A and 12A). Facies Gs strongly dominates forming 73.4% of the relative thickness of FA 1. Occurrence of facies Gm was less common (21.7%), whereas facies Gp was rare. Clast-supported gravels with openwork layers are significantly more common than matrix-supported ones. Pebbles and cobbles are mostly well

ACCEPTED MANUSCRIPT

rounded. Discoidal, bladed or elongated pebbles and cobbles are common. Matrix is poorly sorted coarse to very coarse sand. The thickness of the individual facies set is mostly less than 20 cm.

The erosional base of FA 1 is covered by the coarsest clasts (cobbles and rare boulders up to 45 cm) and the fining upward trend of the beds is typical. The base is mostly almost flat or slightly inclined (<5^{o}); however, in log 3 (Fig. 8) the inclination reaches 18^{o}. The tops are sharp with a broadly convex upwards appearance. Both the imbrication and tilt of the basal surface indicate the main transport towards the ESE or SE. FA 1 overlies the deposits of FA 2 (see Fig. 10A and 12A, B).

Interpretation: FA 1 is interpreted as fluvial deposits (Miall, 1996). Facies Gs, Gm and Gp represent an infill of the fluvial paleochannels (Nemec and Postma, 1993) and the basal enrichment by coarsest clasts is channel-floor lag (Miall, 1996). These channels have been occupied by low-relief longitudinal bars (Nemec, Postma 1993) or by bedload sheets (Whiting et al., 1988). The thickness of the individual facies set points to relatively shallow channels and low relief bars, which is also reflected by the lower role of facies Gp. Similar channels and bars are also developed in the actual stream channels in the modern valley.

4.3.2. FA 2 - Foreset

These sandy and gravelly deposits represent 50% of the logged sections and have been recognised in all of them. FA 2 consists of steeply inclined (20-30^{o}), laterally continuous, sandy to gravelly beds oriented at variable directions (130^{o}-232^{o}). The vertical thickness of FA 2 in sections varies between 125 and 260 cm; however, its base was not always reached due to the collapsing walls of the artificial outcrops. Contact of FA1 and FA2 is generally angular and sharp (see Fig. 10A and

ACCEPTED MANUSCRIPT

12A, B). Deposits of FA 2 cover deposits of FA 3. Their contact is sharp and angular with typical strong reduction of the dip of beds. Tangential contact was not observed.

FA 2 is composed of six lithofacies (Sf, Sl, Sx, Gl, Gmg and Gms); however, only three of them (Sl, Gl and Gms) form the larger portion of the association (Figs. 11A, 12A,B). Plane-parallel sands of (Sl) are the dominant facies and form 52% of the relative thickness of FA 2 (Fig. 8A), plane-parallel gravels (Gl) represent 25% and clast-supported, massive non-graded gravels (Gms) comprise almost 15 % of FA2. Massive, normally graded pebbly sands, granule gravels or pebble gravels of facies Gmg represents about 4%. Solitary backsets of very coarse sand cross-strata dipping upslope of facies Sx (1%) and rhythmic alternation of laminas to thin beds of silty sand or very fine sand and laminas of fine to medium or medium to coarse-grained sand of facies Sf (3%) were recognised in only two sections and one section respectively, where they form about 10 – 30 cm thick beds. Facies Sx fills trough-shaped scours about 15 cm deep. Typical are cross-strata dipping upslope at ca 110-170° relative to the prevalent FA2 bedding.

Two sub-associations can be recognised according to the occurrence of the lithofacies. The first more common sub-association FA2a (outcrops 1, 2, 3 and 5) is composed of facies Sl, Gl, Sx and Sf. The second less common sub-association, FA2b (outcrops 3 and 4), is formed by facies Gms, Gmg and Sl.

Interpretation: The lithofacies assemblage suggests steep delta foresets dominated by deposition of sediment gravity flows (Nemec, 1990). Rare and small chutes or slump scars were infilled by backset (facies Sx). Variations in the direction of the dip of forest (except backset) are explained by existence of several deltaic lobes. The progradation is generally towards S-SW or S-SE and points on the deepest parts of the lake, which were predisposed by the basement morphology.

ACCEPTED MANUSCRIPT

Contact of FA1 and FA2 can be interpreted as oblique toplap geometry (Mitchum et al., 1977; Gobo et al., 2015).

FA2a represents turbidite-dominated foreset deposits and FA 2b debrite-dominated foreset deposits. The different delta-slope sedimentation processes in these two sub-associations reflect the delta-front morphodynamic responses to base-level changes (Gobo et al., 2015). The sedimentation processes within strongly dominant FA2a, together with the erosional oblique toplap, might be attributed to a deficit of the delta-front accommodation (stillstand or fall of water level) and the sediment bypass of the front. FA2b could be attributed to the increased accommodation connected with rising water level, accompanied by storage of sediment along the aggrading delta front, which underwent discrete gravitational collapses. The high proportion of foreset turbidites (see Figs 8-12) can be attributed to a fairly persistent sediment bypass of the delta front due to a deficit of accommodation with a highly limited transient storage of sediment at the delta front (Gobo et al., 2015). However, narrow early-stage bayhead Gilbert-type deltas tend to comprise mainly turbidites within their subaqueous slope deposits in general (Gobo et al., 2014a).

The morphodynamic zone for sediment transfer from topset (dominated by river and basinal regime) and the foreset (dominated by gravitational sediment transport) is known as delta brink zone (Kleinhans, 2005; Gobo et al., 2015). The altitude of the topset/foreset contact did not markedly changed within the terraces and reveal low inclination (2^{o} - 6^{o}) generally towards the S-SE. Recognised subhorizontal to falling delta brink trajectory is connected with delta progradation (Colella, 1988; Dart et al., 1994; Helland-Hansen and Martinsen, 1996; Massari, 1996; Benvenuti, 2003); however, it might be erosionally truncated.

ACCEPTED MANUSCRIPT

The transition from foreset to bottomset connected with gradual reduction of the dip of the forests towards their base was not observed. An exception might be the interbed of facies Sf (which otherwise typically occurs in FA 3) within monotonous steeply inclined succession of lithofacies Sl, recognised in one section (log 2). These deposits might be interpreted as representing delta-toeset to lower delta foreset deposits (Clemmensen and Houmark-Nielsen, 1981; Bornhold and Prior, 1990; Lønne, 1995; Nemec et al., 1999, Winsemann et al. 2007).

4.3.3. FA 3 - Bottomset-Prodelta

Horizontal to subhorizontal (<10^{o}) laterally continuous beds of mainly sand to silty sand with minor occurrence of gravelly interbeds (textural bimodality) are typical features of FA3. These deposits represent 23.5% of the logs and they typically underlay the deposits of FA2 and cover the bedrock or deposits of FA4 (Fig. 8B). They were identified in almost all logged sections (missing in sections 2 and 5, which were relative shallow to reach them). The logged thickness of FA 3 varies between 20 and 205 cm (120 cm in average). Contact of FA2 and FA3 is generally angular and sharp.

FA 3 is composed of six lithofacies (Sf, Sp, Sm, Sr, Sfd and Gm); however, only two of them (Sf and Sfd) form the larger portion of the facies succession. Rhythmites of facies Sf compose the dominant facies (62.4%) and their deformed variant (lithofacies Sfd) is the second most common one (24.4%). The beds of these lithofacies are also thicker (15-60 cm) than the beds of the remaining facies of FA 3. The remaining lihofacies (Sp, Sm, Sr and Gm) form only a few percent each and their beds are typically only a few cm thick. The alternation of thicker bed of finer grained lithofacies Sf or Sfd with thinner beds of coarser grained lithofacies Sm, Sr or Gm is

ACCEPTED MANUSCRIPT

generally typical of FA 3. Occurrence of isolated pebbles (about 5 cm in diameter) is a typical feature of facies Sf.

Two sub-associations can be recognised according to the occurrence of dominant lithofacies (i.e. Sf or Sfd). The first, more common, sub-association FA3a is composed of facies Sf, Sp and Sr (outcrops 1, 2 and 4 – see Fig. 11B). The second sub-association FA3b is formed by facies Sfd, Gm, Sr and Sm (outcrop 3 - see Figs. 10B, C). The deposits of FA3a cover the deposits of FA 4 and are truncated by FA2 (Figs 8, 10, 11). The deposits of FA3b are found in between the deposits of FA3a.

Interpretation: The most common lithofacies Sf results from alternating deposition from suspension and hyperpycnal underflows (low-density turbidity currents – Lowe, 1982). The isolated pebbles are interpreted as dropstones (see Fig. 10B), when clasts were picked up by ice and deposited as ice melted. Their occurrence points mostly to growlers flowing on the lake and indicate that sedimentation took place within an ice-contact lake associated with a calved ice margin (Ravier et al., 2014). Thin interbeds of facies Gm are interpreted as emplaced by gravity flows from the steep delta slopes. These flows might also be responsible for emplacement of some pebbles into lithofacies Sf. Delivery of individual pebbles connected with modification of the debris flows deposits (Postma et al., 1988) is unlikely.

Alternations of deposition from upper and lower flow regime (Sf vs. Sr) or beds with lower and higher coarse bedload delivery (Sm, Sr, Sf vs. Gm) reflect variations in the fluvial discharge and sediment input into the basin. Such variations might reflect spring/summer melting of the snow and ice and autumn/winter paucity of melting water. Similarly, truncated tops of beds indicate that the accommodation available for sediment deposition was suddenly restricted vertically. Recurrent

ACCEPTED MANUSCRIPT

sedimentary pattern, inferred from repetitive changes in sediment supply or temporal changes in flow competence, is often associated with glaciofluvial environments (Knight, 2003; Clerc et al., 2012; Lesemann et al., 2010).

The two recognised facies sub-associations (i.e. FA3a and FA3b) principally show variations in the syn- to early postdepositional deformations. These hydroplastic deformations (convolute bedding, fold structures – see Fig. 10C) in facies Sfd reveal a horizontal transport, related to shear, and indicate deformations imposed by the overriding ice or mobile soft sediment (Eilertsen et al., 2011). In glacial environments, such deformations can be formed in either subglacial or proglacial environments. Here, the deformation structures are limited to individual beds, separated by beds of undeformed deposits. It points to cyclical sediment deformation and coeval sediment deposition (Lesemann et al., 2010; Ravier et al., 2014). The deformations indicate that the space for propagation of sediment deformation is limited, i.e. deformation occurs in a confined environment (Ravier et al., 2014). The deformation structures are typically located directly below coarser grained lithofacies, which truncated the finer grained beds, indicating that deformation predates the deposition from the traction flows. Deformation features were documented in only one log (i.e. log 3 see Fig. 10). This log is typical by relative large thickness of FA3 (comparing to FA 2), the highest occurrence or coarse-grained lithofacies Gm within the FA3 in all logs and important role of FA 2b (i.e. debrite-dominated foreset deposits). The laminae is generally curved in direction of the mass flow movement on foresets. The downslope moving flows provide sufficient shear stress to produce ductile deformations in the underlying beds, which were water saturated (Postma et al., 1983; Pisarska-Jamrozy and Weckert, 2013). Log 3

ACCEPTED MANUSCRIPT

represents relatively shallower part of the lake. Deformation structures related to iceberg keel scouring have not been recognised.

4.3.4. FA 4 - Reworked subglacial deposits

Discontinuous coarse-grained deposits of matrix supported massive pebble to cobble gravel of facies Gmi blanketing the crystalline basement represent FA4 (Fig. 8B). They represent 0.1% of the logs and are covered by the deposits of FA3. They were identified along the base of sedimentary successions of terraces II, III and IV, and are supposed also along base of terrace I. The logged thickness of FA 4 varies between 5 and 7 cm; however, may reach several dm locally. Contact of FA3 and FA4 is irregular and sharp (connected with significant grain size drop - see Fig. 8B).

Interpretation: Discontinuous relatively thin blanket of lithofacies Gmi is interpreted as reworked coarse-grained material form basal debris-rich ice released by melting water which intruded below the glacier (Allaart, 2016). Fine grained material filling the open space between the coarse clasts was delivered by currents of the distal prodelta. Meltout clasts released from the basal debris-rich ice in the subglacial parts of the lake could form some dropstones in the delta bottomset (similarly Bennett et al., 2006). However, the majority of recorded dropstones originated from blocks of ice calved or collapsed into the lake and forming floating iceberg growlers - see Fig. 13 (similarly Lønne, 1995).

4.4. Ground penetrating radar

Two georadar cross sections were measured in the eastern depression (Fig. 2). Cross section R1 shows internal organisation of terrace II and cross section R2 reflects internal organisation of terraces III and IV. Georadar profiles are subdivided

ACCEPTED MANUSCRIPT

into halves for better visual presentation (R1-a, b, R2-a, b - see Fig. 13a,b,c,d). Four main georadar units (GRU) were defined based on the characteristic reflection configuration (parallel to subparallel reflections in each unit).

GRU 1 is characterised by continuous to short discontinuous, horizontal to sub-horizontal, rarely slightly convex upward, parallel reflections. The thickness of GRU 1 did not exceed 75 cm; however, the topmost part of the profile was not recognised by the antenna used. GRU1 always forms the upper most part of the profile. The base of the unit truncates the underlying reflections of GRU 2. GRU 2 is generally characterised by the dominance of gently to steeply inclined reflections. These reflections are generally parallel and dip down-valley. Occasionally, short, horizontal, concave up and concave down reflections occur between more continuous dipping reflections (Fig. 13e). The thickness of GRU 2 ranges from 0.5 to 2 m and its wedge shape can be followed in profile R2-a (Fig. 13d). GRU 3 is generally characterised by mostly continuous, gently dipping (significantly less inclined than reflections of GRU 2) to horizontal reflections. The thickness of GRU 3 ranges from 0.2 m to 1.5m. Transition from GRU 2 into GRU 3 can be observed in the NNW part of the profile R2-b (Fig. 13d). This transition is connected with the gradual passage of inclined reflections to flat laying horizontal ones i.e. gradual decrease of the reflection dip. More complex internal organisation of GRU 3 can be observed in some parts of the profile (Fig. 13b,d). Only the upper parts of GRU 4 were documented by the georadar, whereas its base was not reached. GRU 4 is characterised by convex upward reflections which are either continuous or short. Hyperbolic reflections (white arrow in Fig. 13b) were recognised in profile R1-b within GRU 4.

Interpretation: The comparison of the GPR profiles with sedimentary logs and sections (Fig. 14a,b,c,d) enables the recognition of the relation of the GRU with the

ACCEPTED MANUSCRIPT

above defined FA. GRU 1 corresponds to FA 1 (topset) and its reflections sharply truncate underlying inclined reflections of GRU 2 (Jol and Smith, 1991). GRU 2 corresponds to FA 2 (foreset) (Roberts et al., 2003;Eilertsen et al., 2011). Toplap of inclined reflections of GRU 2 in contact with subhorizontal reflections of GRU 1 reveals the erosional relation of topset and foreset. Variations in the angle of the dip of individual series of inclined reflexions reveal differences in the position of distributive channels on the braided delta plain, or possibly variations in the energy of mass flows on the delta slope. Steeper reflexions are connected with deeper/larger distributive channels or steeper foreset where the more energy is distributed. Flatter reflections are connected with shallower marginal channels. Less common short subhorizontal reflections recognised within series of continuous inclined ones are interpreted as backset, cut and fill (chutes) or slope failure structures (Roberts et al., 2003; Eilertsen et al., 2011). GRU 3 corresponds to FA3 (bottomset) (Jol and Smith 1991; Eilertsen et al., 2011). Downlap of inclined reflection of GRU 2 on flat GRU 3 reveals prograding of foreset onto bottomset. Lateral transition of steeply inclined reflections of the GRU 2 into low-inclined reflections of the GRU 3 (observed in profile R2-b – terrace III) represents lakeward transition of foreset to bottomset i.e. toeset (Eilertsen et al., 2011). GRU 4 is interpreted as the crystalline bedrock, which is confirmed by evidence of bedrock within natural outcrops. Parallel orientation of reflections of GRU 3 and 4 reveals a concordant relation of bedrock surface, bottomset blanketing and overall aggrading pattern. Undulated and terminated reflections (white arrow in Fig. 14) indicate erosive contact of some bottomset beds and might be connected with variations in orientation of hyperpycnal flows (Lønne, 1997; Eilertsen et al., 2011).

ACCEPTED MANUSCRIPT

Variations in thickness and lateral extent of both GRU 3 (bottomset) and GRU 2 (foreset) observed in the GPR profiles are partly attributed to the bedrock morphology. Thicknesses of both bottomset and foreset beds are greater above basement depressions and are significantly reduced above basement hights. Steeper gradient/angle of the dip of GRU 2 can be observed above bedrock depressions if compared to basement elevations in detail. So, according to delta typology the predominant Gilbert type shallow water delta can even transit in some cases to Hjulström type shallow water delta (cf. Postma, 1990), where the subaqueous foreset have about similar gradient as its topset or even to bypass delta (cf. Eilertsen et al., 2011), where foreset is missing. This situation was recognised only in GPR profiles (black arrow in Fig. 13c).

The prograding trend of delta and significant role of basement morphology on deltaic architecture can be well followed in radar profile R2-b (Fig..14d). Reactivation of foreset beds separating several stages of foreset evolution can be recognised above depressions of bedrock (red arrows in Fig.13d). Both relative deepening of the lake and lake level drop follow the transition of the lake over steps of bedrock. The feeding meltwater stream incised into the delta plain and foresets prograded lakeward. The R2-b profile illustrates two such situations (grey and black arrows in Fig. 14d) with reactivation of forest beds and stream incision.

A direct relation existed between terrace levels and bedrock relief. Flat terrace surfaces coincide generally with flat parts of the bedrock and steep terrace scarps with the inclined parts of the bedrock.

5. Discussion

ACCEPTED MANUSCRIPT

Facies analysis proved the existence of a “classical” tripartite Gilbert-type delta (Gilbert, 1885; Kleinhans, 2005; Nemec, 1990), which prograded into the lake and towards the glacier. Well developed, short and steep delta foresets, and relatively thick and extended bottomset both confirm rapid aggradation and progradation of the Gilbert delta into a basin, reflect a high basin/river depth ratio; as the delta thickness depends on the basin accommodation. The further important factors for formation of a steep delta profile are sufficient bedload and spreading of the effluent as an axial turbulent jet (Postma, 1995; Eilertsen et al., 2011). Relation of the channel depth to basin depth immediately basinward of the river mouth is expressed as a depth ratio (sensu Jopling, 1965). The depth ratio in the studied case varies between 0.2 and 0.5, which correspond to the development of steep delta foresets.

The identified topset-foreset boundary was used as a lake-level indicator for determination of the palaeodepth corresponding approximately to the delta rim during deposition (Eilertsen et al., 2011). Observed situation on the incised stream shows that the feeding stream was probably not deeper than one meter. The erosional topset-foreset boundary might be formed in a slightly greater depth and could reflect erosion of the foreset. Based on this assumption we can suppose depth of the lake of about 5 – 6 m.

The deltaic wedges thicken in the lakeward direction and reflect subaerial bypass and lakeward transfer of sediment, as well as high efficiency of sediment dispersal. The downstream fining pattern (topset-foreset-bottomset) points to the important role of suspended load in the total load (Jopling, 1965). The lateral and upward grain-size variations together with direction of the forest dip reflect delta progradation generally towards the south.

ACCEPTED MANUSCRIPT

Water input was realized by a feeding stream entering the eastern depression, whereas the western depression played an important role for the water output and relative stability of the lake level (in periods between the ice dam collapses). The bedrock morphology confined the stream trunk to a narrow gorge, forming a point source and single dominant sedimentary influx point.

The relationship between accommodation and sediment supply is used to understand paleogeographical changes (Emery and Myers, 1996; Catuneanu et al., 2011). Accommodation is defined as the space available for sediments to fill (Jervey 1988) and may be modified by the interplay between climate, tectonism, energy flux, sea-level changes and sedimentation (Catuneanu et al., 2011). Shoreline trajectory and shoreline-related stacking patterns are crucial for the understanding of the interplay of available accommodation and sediment supply at syn-depositional time (Helland-Hansen and Gjelberg, 1994; Helland-Hansen and Martinsen, 1996; Catuenanu et al., 2011).

The recognised fluvio-deltaic terraces proved four rapid lake level falls, followed by fluvial downcutting, erosion and redeposition of the older deltaic deposits, the shifting of the lake position towards the damming glacier and transition of the sediment input basinward. The thickness and lakeward extent of the deltaic wedges are thought to reflect the lake accommodation (local water depth) and the rate of sediment supply (stream discharges). The glacier dam retreat and the basin floor morphology are supposed to be the responsible factors for the recognised forestepping and downstepping stacking pattern (regressive regime) and also led to final lake termination, due to a subglacial burst of the ice-dam and opening of the lake outlet.

ACCEPTED MANUSCRIPT

Forestepping and downstepping at the lake shoreline, fluvial downcutting with erosion and redeposition of previously deposited sediment are interpreted as a specific type of shoreline trajectory i.e. forced regression, which is connected with negative accommodation (i.e. reduction/deficiency of the space to accumulate sediment - Helland-Hansen, Hampson 2009, Catuneanu et al. 2011) typically joined with lake level fall and reduction of the water volume. However, accommodation in lacustrine basins is not limited by the lake water volume only, but is also controlled by the sediment accumulation rate and basin topography. The limited water volume and relatively small lake depth render lakes highly sensitive to changes in basin floor configuration (Ilgar, Nemec 2005).

Each lake level fall is connected with collapse of existed ice-dam and rapid shift/retreat of the dam to a new position. The rapid shift of the lake position and extent occurred above the stepped bedrock, which was inclined generally in the direction of glacier retreat, in combination with relative broadening and flattening of the gorges towards the damming glacier and highly localized sediment supply. A general increase of lake water volume and depth in time for the studied lake is a result of above mentioned combination of variables. Ice dam failure led to abrupt change in the lake level (Fig. 15a-e). Lake level fall influenced the base level, which was reflected by change of the stream profile. The stream profile was readjusted to the new lake level by cutting into the former sedimentary infill, promoting a valley incision and the deposition of forced regressive coarse-grained delta wedges in front of the valley. Valley incision was typical for the marginal portions of the lake. The deposition promoted during decreasing rates of lake-level fall and its relative stability, because the alluvial gradient was larger than the emergent lake profile and so alluvial

ACCEPTED MANUSCRIPT

aggradation occurs (Schumm, 1993; Blum and Törnqvist, 2000; Muto and Steel, 2004; Petter and Muto, 2008; Winsemann et al.2011).

The incision of the feeding stream led to partial erosion and redeposition of the former deposits. This redeposition might temporarily increase the sediment supply. Similarly cyclic/seasonal variations in the meltwater discharge (ruled by climatic conditions) affected both the lake water budget and the catchment sediment yield. These variations were less important (both spatially and volumetrically), when glacier retreat and basement morphology. Moreover, whereas the deposition in the eastern depression was ruled by glacier retreat, basement morphology and rate of sediment supply, only the roles of glacier retreat and basement morphology are supposed to govern the deposition in the western depression. The reason is the limited sediment input into this depression. The intrabasinal bedrock ridge prevented the entrance of the delta into the western depression and maintained the delta in the relatively narrow eastern depression for the whole period of the lake evolution. Therefore both depressions reveal different infill and depositional style. The satellite image from the year 2009 demonstrates significantly larger water extent in the western depression, whereas the water table in the eastern depression was developed only along the glacier margin itself (see Fig. 5).

Alternation of sub-associations 2a and 2b, similarly like evidence of sub-associations 3a and 3b reveal fluctuation in the lake level (governed probably by variations in the meltwater discharge and sediment supply). Similarly Gobo et al. (2015) suggest that debrite-dominated assemblages vs. turbidite-dominated assemblages reveal variations in accommodation and sediment storage.

In the lake terrace systems, commonly the highest terrace is connected with maximum lake level for the prograding delta front (Eilertsen et al., 2011). However, in

ACCEPTED MANUSCRIPT

the studied case the largest areal extent was recognised for the lowest and youngest terrace IV. The reason is the basement morphology. Deposits of terrace IV are located above a relatively broad bowl shaped depression where stepped scarps and internal bedrock elevations are missing (Figs. 13a,b,c,d; 15d). Moreover, the fluvial erosion and downcutting affected the preserved extent of older terraces.

Conceptual models of ice-dammed lakes are mostly for lakes dammed by a stable glacier front or for lakes formed during glacier advance (Winsemannn et al., 2004, 2007; Salamon et al., 2013). Both a general lake level rise and an aggradational regime (with episodic oscillations) are typical of such lakes. The proposed study is “purely deglacial” and can be compared to stratigraphic style F_s (overall fall with periods of standstill and no significant rises) sensu Postma (1995).

The lack of strandplain/beach facies is characteristic of the studied case, which can be explained by several reasons: i) rapid intense sediment delivery to the delta rim, inducing delta progradation and preventing the development of shoreline processes; ii) the both areal and time restricted extent of the lake could propose restricted time for formation and preservation of beach facies. Similar lake evolution can be generally expected in lakes connected with kames especially in morphologically indented relief of the submontaneous areas.

Sediment delivery in ice-contact glacial lakes is documented mostly by torrential subglacial streams directly from the glacier (Clemmensen and Houmark-Nielsen, 1981; Mastalerz 1990; Winsemannn and Asprion 2001). The studied lake reveals a continuously opposite direction of the feeding stream sediment delivery i.e. towards the damming glacier.

The mean linear retreat rate of Nordeskiöldbreen in the study area can be derived in detail from the extent of the glacier on available images. Such an

ACCEPTED MANUSCRIPT

evaluation shows that from 1961 till 1990 the glacier retreated about 90 m (3m/a). From 1990 till 2009 the glacier retreated about 160 m (8m/a). Finally, from 2009 till 2015 the glacier retreated about 40 m (7m/a). The observed more rapid retreat of the glacier front between the years 1990 – 2015 is connected with the ice calving into the lake. The existence of the lake and drainage of its water below the glacier significantly enlarged the rate of local deglaciation.

6. Conclusions

Deposits of a recent small ice-dammed lake have been recognised along the margin of Nordenskiöldbreen on the northern coast of Adolfbukta, central Spitsbergen, Svalbard. The evolution of the lake and its deltaic infill is documented based on a detailed lithofacies analysis of the artificial outcrops, ground penetrating radar data, study of satellite images and photos of the glacier front and landscape mapping by drone.

Two depressions formed along tight and relatively deep gorges predisposed by structural lines in the crystalline basement and oriented perpendicularly to the margin of the glacier. These two depressions were occupied by the studied lake and they were partly separated by a flat rock ridge. While the eastern depression is narrow and elongated, the western depression is more opened. The eastern depression is almost filled by deltaic deposits with four morphologically distinct terraces on the surface. The western depression contains only a thin sedimentary blanket. The feeding stream entered directly into the eastern depression and the western depression did not have its own direct fluvial feeder and was subsidized by both water and sediment from the eastern depression. The lake formed between the years 1990 – 2000 and terminated between the years 2009-2012. The maximum depth of

ACCEPTED MANUSCRIPT

the lake was about 5 m. The observed average glacier dam retreat in the area of the lake was 7-8 m/a.

The lake was filled by deposits of a “classical” tripartite Gilbert-type delta, which in general reveals a high basin/river depth ratio. Lithofacies have been grouped into four different facies associations corresponding to four different depositional environments. The majority of these environments generally correspond to a tripartite (Gilbert-type) delta zones: topset (FA1), foreset (FA2) and bottomset (FA3) filling a proglacial lake. The remaining FA 4 represents reworked subglacial deposits. The sedimentary infill represents terminoglacial coarse-grained glacilacustrine deposition in an undulated relief. Basement morphology affected the depositional architecture of the delta. The thicknesses of both bottomset and foreset are greater above basement depressions and are significantly reduced above basement elevations.

The recognised fluvio-deltaic terraces proved four lake level falls followed by fluvial downcutting, erosion and redeposition of the older lake deposits, shifting of the lake position towards the damming glacier and transition of the sediment input basinward. The glacier dam retreat and the basin floor morphology, tilted towards the glacier, are supposed to be the primary factors for the recognised forestepping and downstepping stacking pattern. They also led to final lake termination.

The studied lake deposits may serve as an interesting case study for the lake sequence stratigraphic models because it was connected only with glacier retreat (overall lake level fall with periods of standstill and no significant rises). Moreover, the direction of the feeding stream of the lake and the delta progradation was continuously towards the damming glacier. These are the principal differences to the proposed models of ice-dammed lake (Salamon et al., 2013; Winsemann et al., 2004, 2007, 2011).

ACCEPTED MANUSCRIPT

Acknowledgements

The work was supported by the Ministry of Education, Youth and Sports (MEYS) large infrastructure project LM2015078 “Czech Polar Research Infrastructure”. We are obliged to thank Grzegorz Rachlewicz (Adam Mickiewicz University, Poznań) for providing historic photos of Nordenskiöldbreen and satellite imagery of the year 1990. We thank Petra Polická and Martin Hais (University of South Bohemia, České Budějovice), and Lenka Ondráčková (Masaryk University) for providing of further satellite images. We also thank participants of the “Polar Ecology Course - Geosciences“, which was organised in the year 2015 by Masaryk University, Brno, for their help with the field works and to the Czech Arctic Research Infrastructure *“Josef Svoboda Station”* (as a part of the Czech Polar Research Infrastructure, CzechPolar2) and its crew for their support. We also would like to thank Katarina Gobo and an anonymous reviewer for their helpful comments and suggestions, which highly improved the quality of the paper. We thank Markus Stoffel for editing the manuscript.

References

Aitken, J.F.,1995. Lithofacies and depositional history of a Late Devensian ice-contact deltaic complex, northeast Scotland. Sedimentary Geology, 99, 111-130.

Allaart, L., 2016. Combining terrestrial and marine glacial archives: A geomorphological map of the Nordenskiöldbreen forefield, Svalbard. Ph.D. Thesis, Norwegian University of Science and Technology, Norwey.

ACCEPTED MANUSCRIPT

Benvenuti, M., 2003. Facies analysis and tectonic significance of lacustrine fan-deltaic successions in the Pliocene-Pleistocene Mugello Basin, Central Italy. Sedimentary Geology, 197-234.

Bennett, M. R., Huddart, D., Waller, R. I., 2006. Diamict fans in subglacial water-filled cavities – a new glacial environment. Quaternary Science Reviews, 25, 3050–3069.

Blum, M.D., Törnqvist, T.E., 2000. Fluvial responses to climate and sea-level change: a review and look forward.Sedimentology, 47, Suppl.1, 2-48.

Boothroyd, J.C., Ashley, G.M., 1975. Processes, bar morphology, and sedimentary structures on braided outwash fans, northeastern Gulf of Alaska. In: Jopling, A.V., McDonald B.C. (Eds.), Glaciofluvial and Glaciolacustrine Sedimentation. SEPM Spec. Publ., 23, pp. 193–222.

Bornhold, B.D., Prior, D.B., 1990. Morphology and sedimentary processes on the subaqueous Noeick River delta, British Columbia, Canada. In: Colella, A., Prior, B.D. (Eds.), Coarse-Grained Deltas. Spec. Publ. of IAS, 10, pp.169-181.

Catuneanu, O., Galloway, W.E., Kendall, C.G.St.C., Miall, A.D., Posamentier, H.W., Strasser, A., Tucker, M.E., 2011. Sequence Stratigraphy: Methodology and Nomenclature. Newsletters on Stratigraphy, 44/3, 173-245.

Clark, P.U., Marshall, S.J., Clarke, G.K.C., Hostetler, S.W., Licciardi, J.M., Teller, J.T., 2001. Freshwater forcing of abrupt climate change during the last glaciation. Science 293, 283-287.

Clemmensen, L., Houmark-Nielsen, M., 1981. Sedimentary features of a Weichselian glaciolacustrine delta. Boreas,10, 3, 229-245.

ACCEPTED MANUSCRIPT

Clerc, S., Buoncristiani, J.F., Guiraud, M., Desaubliaux, G., Portier, E., 2012. Depositional model in subglacial cavities, Killiney Bay, Ireland. Interactions between sedimentation, deformation and glacial dynamics. Quatern. Sci. Rev., 33, 142–164.

Colella, A., 1988. Pliocene-Holocene fan deltas and braiddeltas in the Crati Basin, southern Italy: a consequence of varying tectonic conditions. In: Nemec W., Steel R.J. (Eds.) Fan Deltas: Sedimentology and Tectonic Settings. pp. 50–74. Blackie, London.

Dallmann, W. K., Piepjohn, K., Blomeier D., 2004. Geological map of Billefjorden, Central Spitsbergen, Svalbard with geological excursion guide. Temakart Nr. 36. Norsk Polarinstitutt.

Dart, C.J., Collier, R.E.L., Gawthorpe, R.L., Keller, J.V.A., Nichols, G., 1994. Sequence stratigraphic of (?)Pliocene-Quaternary synrift, Gilbert-type fan deltas, northern Peloponnesos, Greece. Mar. Petrol. Geol., 11,545–560.

Donnelly, R., Harris, C., 1989. Sedimentology an origin of deposits from a small ice-dammed lake, Leirbreen, Norway. Sedimentology, 36, 581-600.

Eilertsen, R.S., Corner, G.D., Aasheim, O., Hansen, L., 2011. Facies characteristics and architecture related to palaeodepth of Holocene fjord–delta sediments. Sedimentology 58, 7, 1784-1809.

Emery, D., Myers, K. J., 1996. Sequence Stratigraphy. Oxford, U.K., Blackwell, 297 pp.

Evans, D. J. A., Strzelecki, M., Milledge, D. G., Orton, C., 2012. Hørbyebreen polythermal glacial landsystem, Svalbard. Journal of Maps: 8 (2): 146–156. DOI: 10.1080/17445647.2012.680776

ACCEPTED MANUSCRIPT

Ewertowski, M.W., Evans, D.J.A., Roberts, D.H., Tomczyk, A.M., 2016. Glacial geomorphology of the terrestrial margins of the tidewater glacier, Nordenskiöldbreen, Svalbard. Journal of Maps 12, 1, 476–487. DOI: 10.1080/17445647.2016.1192329

Fisher, T.G., Clague, J.J., Teller, J.T., (Eds.) 2002. The role of outburst floods and glacial meltwater in subglacial and proglacial landform genesis, The role of outburst floods and glacial meltwater in subglacial and proglacial landform genesis. Quaternary International 90, pp. 1-115

Gilbert, G.K.,1885. The topographic features of lake shores.US Geol. Surv. Ann. Rep., 5, 69–123.

Giosan, L., Bhattacharya, J.P., (Eds.) 2005. River deltas – concepts, models and examples. SEPM Spec. Publ. 83, pp. 1-502.

Gobo, K., Ghinassi, M., Nemec, W. Sjursen, E., 2014a. Development of an incised valley-fill at an evolving rift margin: Pleistocene eustasy and tectonics on the southern side of the Gulf of Corinth, Greece. Sedimentology, doi: 10.1111/sed.12089.

Gobo, K., Ghinassi, M., Nemec, W., 2014b. Reciprocal changes in foreset to bottomset facies in a Gilbert-type delta: response to short-term changes in base level. J. Sed. Res., 84, 1079–1095.

Gobo, K., Ghinassi, M., Nemec, W., 2015. Gilbert-type deltas recording short-term base-level changes: Delta-brink morphodynamics and related foreset facies. Sedimentology, 62, 1923-1949.

Hambrey, M. J., Glasser, N. F., 2012. Discriminating glacier thermal and dynamic regimes in the sedimentary record. Sedimentary Geology 251-252: 1-33.

Heinz, J., Aigner, T., 2003. Three-dimensional GPR analysis of various Quaternary gravel-bed braided river deposits (southwestern Germany). In: Bristow,

ACCEPTED MANUSCRIPT

C.S., Jol, H.M. (Eds.), Ground Penetrating Radar in Sediments. Geological Society, London, Special Publications, 211, pp. 99-110.

Helland-Hansen, W., Gjelberg, J. G., 1994. Conceptual basis and variability in sequence stratigraphy: a different perspective. Sedimentary Geology, 92, 31-52.

Helland-Hansen, W., Hampson, G.J., 2009. Trajectory analysis: concepts and applications. Basin Research , 21, 5, 454-483

Helland-Hansen, W., Martinsen, O.J., 1996. Shoreline Trajectories and Sequences: Description of Variable Depositional-Dip Scenarios. Journal of Sedimentary Research, Section B: Stratigraphy and Global Studies, 66/4, 670-688.

Hornung, J.J., Asprion, U., Winsemannn, J., 2007. Jet-efflux deposits of a subaqueous ice-contact fan, glacial Lake Rinteln, northwestern Germany. Sedimentary Geology 193, 167-192.

Huggenberger, P., 1993. Radar facies: recognition of facies patterns and heterogeneities within Pleistocene Rhine gravels, NE Switzerland. In: Best, J.L., Bristow, C.S. (Eds.), Braided Rivers. Geological Society, London, Special Publications, 75, pp. 163-176.

Ilgar, A., Nemec, W., 2005. Early Miocene lacustrine deposits and sequence stratigraphy of the Ermenek Basin, Central Taurides, Turkey. Sedimentary Geology, 173: 233-275.

Jervey, M.T., 1988. Quantitative geological modeling of siliciclastic rock sequences and their seismic expression. In: Wilgus, C. K., Hastings, B. S., Kendall, C. G. St. C., Posamentier, H.W., Ross, C. A., Van Wagoner, J. C. (Eds.), Sea Level Changes – An Integrated Approach. SEPM Special Publication, 42, pp. 47–69.

ACCEPTED MANUSCRIPT

Johnsen, T.J., Brennand T.A., 2006. The environment in and around ice-dammed lakes in the moderately high relief setting of the southern Canadian Cordillera. Boreas, 35**,** 1**,** 106–125.

Jol, H. M., Smith, D.G., 1991. Ground penetrating radar of northern lacustrine deltas. Can. J. Earth Sci. 28, 1939–1947.

Jopling, A.V., 1965. Hydraulic factors controlling the shape of laminae in laboratory deltas. Journal of Sedimentary Petrology, 35, 4, 777-791.

Kleinhans, M.G., 2005. Autogenic cyclicity of foreset sortingin experimental Gilbert–type deltas. Sedimentary Geology, 18, 215–224.

Kłysz, P., Lindner, L., Makowska, A., Marks, L., Wysokiński, L., 1988. Late Quaternary glacial episodes and sea level changes in the northeastern Billefjorden region, Central Spitsbergen. Acta Geologica Polonica 38 (1-4): 107-123.

Knight, J., 2003. Subglacial and proglacial lake floods. Sedimentary Geology 160, 289-290.

Lang, J., Winsemann, J.,2013. Lateral and vertical facies relationships of bedforms deposited by aggrading supercritical flows: From cyclic steps to humpback dunes. Sedimentary Geology, 296, 36-54.

Lesemann, J.E., Aslop, G.I.,Piotrowski, J.A., 2010. Incremental subglacial meltwater sediment deposition and deformation associated with repeated ice-bed decoupling: a case study from the Island of Funen, Denmark. Quatern. Sci. Rev., 29, 3212–3229.

Lønne, I., 1995. Sedimentary facies and depositional architecture of ice-contact glaciomarine systems. Sedimentary Geology, 98, 13–43.

Lønne, I., 1997. Facies characteristics of a proglacial turbiditic sandlobeat Svalbard. Sedimentary Geology, 109, 13–35.

ACCEPTED MANUSCRIPT

Lowe, D.R., 1982. Sediment gravity flows: II. Depositionalmodels with special reference to the deposits of high–density turbidity currents. Journal of Sedimentary Petrology, 52, 279–297.

Magilligan, F.J., Gomez, B., Mertes, L.A.K., Smith, L.C., Smith, N.D., Finnegan, D., Garvin, J.B., 2002. Geomorphic effectiveness, sandur development, and the pattern of landscape response during jökulhlaups: Skeidararsandur, southeastern Iceland. Geomorphology, 44, 95-113.

MALÅ GeoScience. 2005. Ramac GPR^{TM}. Hardware manual. Malå, GeoScience.

Massari, F., 1996. Upper–flow–regime stratification types onsteep–face, coarse–grained, Gilbert–type progradationalwedges (Pleistocene, southern Italy). Journal of Sedimentary Research, 66,364–375.

Mastalerz, K., 1990. Diurnally and seasonally controlledsedimentation on a glaciolacustrine foreset slope: anexample from the Pleistocene of eastern Poland. In: Colella, A., Prior, D.B. (Eds.), Coarse-Grained Deltas. Spec. Publ. of IAS, 10, pp. 297–309.

Martini, I. P.,1990. Pleistocene glacial fan deltas in southem Ontario, Canada. In Colella, A., Prior, D. B. (Eds.), Coarse-grained Deltas. Spec. Publ. of IAS, 10, pp. 281-295.

Miall, A.D., 1996. The Geology of Fluvial Deposits: Sedimentary Facies, Basin Analysis, and Petroleum Geology. Springer-Verlag, Berlin, 582 pp.

Mitchum, R.M., Vail, P.A. and Sangree, J.B., 1977. Seismic stratigraphy and global changes of sea level; Part 6: stratigraphic interpretation of seismic reflection patterns in depositional sequences. In: Payton C.E. (Ed.), Seismic Stratigraphy Application to Hydrocarbon Exploration. Mem. AAPG, 26, pp. 117–133.

ACCEPTED MANUSCRIPT

Mulder, T., Alexander, J., 2001. The physical character of subaqueous sedimentary density fows and their deposits. Sedimentology, 48, 269-299.

Muto, T., Steel, R.J., 2004. Autogenic response of fluvial deltas to steady sea-level fall: implications from flume-tank experiments. Geology, 32, 401-404.

Nemec, W., 1990. Aspects of sediment movement on steep delta slopes. In: Colella, A., Prior, D.B. (Eds.), Coarse-grained Deltas. Spec. Publ. of IAS, 10, pp. 29-73.

Nemec, W., 2005. Principles of lithostratigraphic logging and facies analysis.- Institutt for geovitenskap, pp. 1-28; Bergen.

Nemec, W., Lønne, I., Blikra, L.H., 1999. The Kregnes moraine in Gaudalen, west-central Norway: anatomy of a Younger Dryas proglacial delta in a paleofjord basin. Boreas, 28, 454-476.

Nemec, W., Postma, G., 1993. Quaternary alluvial fans in southwestern Crete: sedimentation processes and geomorphic evolution. In: Marzo, M., Puigdefabregas, C., (Eds.), Alluvial Sedimentation. Spec. Publ.of IAS, 17, pp. 235-276.

Petter, A.L., Muto, T., 2008. Sustained alluvial aggradation and autogenic detachment of the alluvial river from the shoreline in response to steady fall of relative sea-level. J. Sediment. Res., 78, 98-111.

Pisarska-Jamrozy, M., Weckwerth, P., 2013. Soft-sediment deformation structures in a Pleistocene glaciolacustrine delta and their implications for the recognition of subenvironments in delta deposits. Sedimentology, 60, 637-665.

Postma, G., 1990. Depositional architecture and facies ofriver and fan deltas: a synthesis. In: Colella A., Prior D.B. (Eds.), Coarse–Grained Deltas. Spec. Publ. of IAS, 10, pp. 13–27.

ACCEPTED MANUSCRIPT

Postma, G., 1995. Causes of architecture variation in deltas. In: Oti M.N., Postma, G., (Eds.), Geology of Deltas. pp. 3-16.Balkema, Rotterdam, Netherlands.

Postma, G., Nemec, W. and Kleinspehn, K., 1988. Large floating clasts in turbidites: a mechanism for their emplacement. Sedimentary Geology, 58, 47–61.

Postma, G., Roep, T.B., Ruegg, H.J. 1983.Sandy-gravelly mass-flow deosits in an ice-marginal lake (Saalian, Leuvenumsche Beek valley, Veluwe, the Netherlands), with emphasis on plug-flow deposits. Sedimentary Geology, 34, 59-82.

Rachlewicz, G., Szczuciński, W., Ewertowski, M., 2007. Post- „Little Ice Age“ retreat rates of glaciers around Billefjorden in central Spitsbergen, Svalbard. Polish Polar Research 28 (3), 159–186.

Ravier, E., Buonscristiani, J.F, Clerc, S., Guiraud, M., Menzies, J., Portier, E., 2014. Sedimentological and deformational criteria for discriminating subglaciofluvial deposits from subaqueous ice-contact fan deposits: A Pleistocene example (Ireland). Sedimentology 61, 5, 1382-1410 . doi: 10.1111/sed.12111

Roberts, M.C., Niller, H.-P., Helmstetter, N., 2003. Sedimentary architecture and radar facies of a fan delta, Cypress Creek, West Vancouver, British Columbia. In: Bristow, C.S., Jol, H.M. (Eds.), Ground Penetrating Radar in Sediments. The Geological Society London, Bath, UK, pp. 111–126.

Russell, A.J., 2007. Controls on the sedimentology of an ice-contact jökulhlaup-dominated delta, Kangerlussuaq, west Greenland. Sedimentary Geology 193, 131-148.

Russell, A.J., 2009. Jökulhlaup (ice-dammed lake outburst flood) impact within a valley-confined sandur subject to backwater conditions, Kangerlussuaq, West Greenland. Sedimentary Geology, 215, 33-49.

ACCEPTED MANUSCRIPT

Russell, H.A.J., Arnott, R.W.C., 2003. Hydraulic-jump and hyperconcentrated flow deposits of a glaciogenic subaqueous fan: Oak Ridge Moraine, southern Ontario, Canada. Journal of Sedimentary Research, 73, 887–905.

Salamon, T., Krzyszkowski, D., Kowalska, A., 2013. Development of Pleistocene glaciomarginal lake in the foreland of the Sudetes (SW Poland). Geomorphology, 190, 1–15.

Sandmeier, K.J., 2012. REFLEXW Version 7.0. Karlsruhe, K.J. Sandmeier.

Schumm, S.A., 1993. River response to baselevel change: implications for sequence stratigraphy. J. Geol., 101, 279-294.

Shaw, J., 2002. The meltwater hypothesis for subglacial bedforms. Quaternary International 90, 5 – 22.

Stacke, V., Mida, P., Lehejček, J., Tóthová, G., Nývlt, D., 2013. Recent landscape changes in terminoglacial area of the Nordenskiöldbreen, central Spitsbergen, Svalbard. Czech Polar Reports, 3/1, 3-6.

Stuchlík, R., Stachoň, Z., Láska, K., Kubíček, P., 2016. Unmanned Aerial Vehicle – Efficient Mapping Tool Available for Recent Research in Polar Regions. Czech Polar Reports, 5/2, 210-221.

Talling, P.J., Masson, D.G., Sumner, E.J., Malgesini, G., 2012.Subaqueous sediment density flows: Depositional processes and deposit types. Sedimentology, 59, 1937-2003.

Teller, J.T., 1995. History and drainage of large icedammed lakes along the Laurentide Ice Sheet. Quart. Int., 28, 83-92.

Teller, J.T., Leverington, D.W., Mann, J.D., 2002. Freshwater outbursts to the oceans from glacial Lake Agassiz and their role in climate change during the last deglaciation. Quaternary Science Reviews 21, 879-887.

ACCEPTED MANUSCRIPT

Tucker, M., (Ed.) 1988. Techniques in Sedimentology, pp. 1-394, Blackwell Science.

Walker, R.G., James, N.P., 1992. Facies Models. Response to sea level changes. Geol. Ass. Canada, 1-380; Toronto.

Whiting, P.J., Dietrich, W.E., Leopold, L.B., Drake, T.G., Shreve, R.L., 1988. Bedload sheets in heterogeneous sediment. Geology, 16, 105-108.

Winsemann, J., Asprion, U., 2001. Glazilakustrine Deltas am Südhangdes Wesergebirges: Aufbau, Entwicklung und Kontrollfaktoren. Geol. Beitr. Hannover, 2, 139–157.

Winsemann, J., Asprion, U., Meyer, T., 2004. Sequence analysis of early Saalian glacial lake deposits (NW Germany): evidence of rapid local ice margin retreat and related calving processes. Sedimentary Geology, 165, 223–251.

Winsemannn, J., Asprion, U., Meyer, Z., Schramm, C., 2007. Facies characteristics of Middle Pleistocene (Saalian) ice-margin subaqueous fan and delta deposits, glacial Lake Leine, NW Germany. Sedimentary Geology, 193, 105-129.

Winsemann, J., Brandes, C., Polom, U., 2011. Response of a proglacial delta to rapid high-amplitude lake-level change: an integration of outcrop data and high-resolution shear wave seismics. Basin Research, 23, 22-52.

http://toposvalbard.npolar.no/, 27. 11. 2016.

ACCEPTED MANUSCRIPT

Figure captions:

Fig. 1. Geographic location of the area under study. Source of map - http://toposvalbard.npolar.no/.

Fig. 2. Ortho-photo mosaic of the study area created in July 2016 by UAV (Unmanned Aerial Vehicle) - notice the morphology of the area, position of the depressions, orientation of the feeding stream, position of the outlet, positions of the geoaradar profiles (R1, R2), artificial outcrops with logs (1-5) and fluvio-deltaic terraces in the eastern depression (I-IV).

Fig. 3. The eastern depression with position of four morphologically distinct fluvio-deltaic terraces.

Fig. 4. Evolution of the studied lake and Nordenskiöldbreen front on the satelite images and photos. Red arrow - eastern depression; green arrow - western depression; white arrow - outflow along the intrabasinal ridge. Notice well developed terrace IV in the year 2005 (Fig. 12c). Photo - Grzegorz Rachlewicz.

Fig. 5. Growlers on the lake documented in the year 2009. Source of image: http://toposvalbard.npolar.no/

Fig. 6. Newly (situation in July 2015) formed glaciomarine coarse-grained delta along the NW margins of Adolfbukta in front of Nordenskiöldbreen.

Fig. 7. Schematic reconstruction of the deglaciation along the margin of Nordenskiöldbreen on northern coast of Adolfbukta with evolution of the ice-dammed lake and fluvio-deltaic terraces. Map source - http://toposvalbard.npolar.no/.

Fig. 8. Sedimentological log of the lake sedimentary infill from artificial outcrop 1 with examples of selected lithofacies and facies associations. A) Foreset deposits - lithofacies Sl. The length of the measuring stick is 22cm. B) Bottomset deposits (lithofacies Sp) and cobble of reworked coarse-grained subglacial debris (lithofacies

ACCEPTED MANUSCRIPT

Gmi). The length of the shovel is 50 cm. The log shows the stratigraphic distribution of sedimentary facies (letter code as in Table 1 and distinction of facies associations (FA 1- 4).

Fig. 9. Sedimentological log of the lake sedimentary infill from artificial outcrop 2. A) Overview of the section showing thick succession of the foreset deposits (FA 2).

Fig. 10. Sedimentological log of artificial outcrop 3 with examples of selected lithofacies and facies associations. A) Topset deposits (lithofacies Gm), B) Bottomset lithofacies (arrow points to dropstone). The length of the measuring stick is 1 m., C) Detail of bottomset deposits (deformation structures - lithofacies Sfd). The length of the measuring stick is 22cm.

Fig. 11. Sedimentological log of artificial outcrop 4 with examples of selected lithofacies and facies associations A) Foreset deposits (lithofacies Gms nad Gmg). The length of the measuring stick is 22cm., B) Bottomset deposits (lithofacies Sf and Sr). The length of the shovel is 50 cm.

Fig. 12. Sedimentological log of artificial outcrop 5 with examples of selected lithofacies and facies associations A) Topset and foreset deposits (note angular and erosive contact). The length of the measuring stick is 1 m. B) Foreset deposits (lithofacies Gl and Sl). The length of the measuring stick is 0.9 m.

Fig. 13. Ground penetrating radar profiles across the fluvio-deltaic terraces at Nordenskiöldbreen (both raw data and interpretation) illustrating delta topset (GRU1), foreset (GRU2), bottomset (GRU3) and crystalline bedrock (GRU4). a) south-eastern part of the profile R1, b) north-western part of the profile R1, c) south-eastern part of the profile R2, b) north-western part of the profile R2, e) detail of reflections of GRU 2 and GRU3. Notice occurrence of short, horizontal, concave up and concave down

ACCEPTED MANUSCRIPT

reflections between more continuous parallel and down-valley dipping reflections, which are interpreted as result of backset, chute and pools or slope failure structures.

Fig. 14. Sections of fluvio-deltaic terraces: a) section of terraces II and III, b) section of terrace IV, c) section of terrace II, d) section of terrace IV (right side of the river cut). E) section of the terrace IV (left side of the river cut).

Fig. 15. Schematic reconstruction of the retreat of Nordenskiöldbreen glacier with formation of system of fluvio-deltaic terraces and shifting of the lake position.

ACCEPTED MANUSCRIPT

ACCEPTED MANUSCRIPT

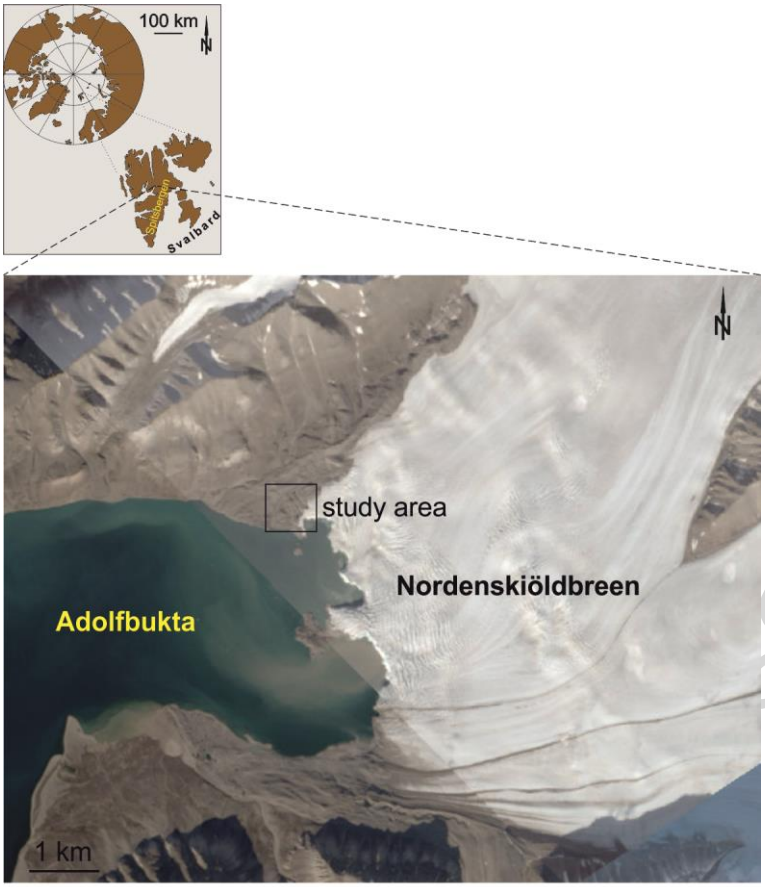

Fig.1

ACCEPTED MANUSCRIPT

ACCEPTED MANUSCRIPT

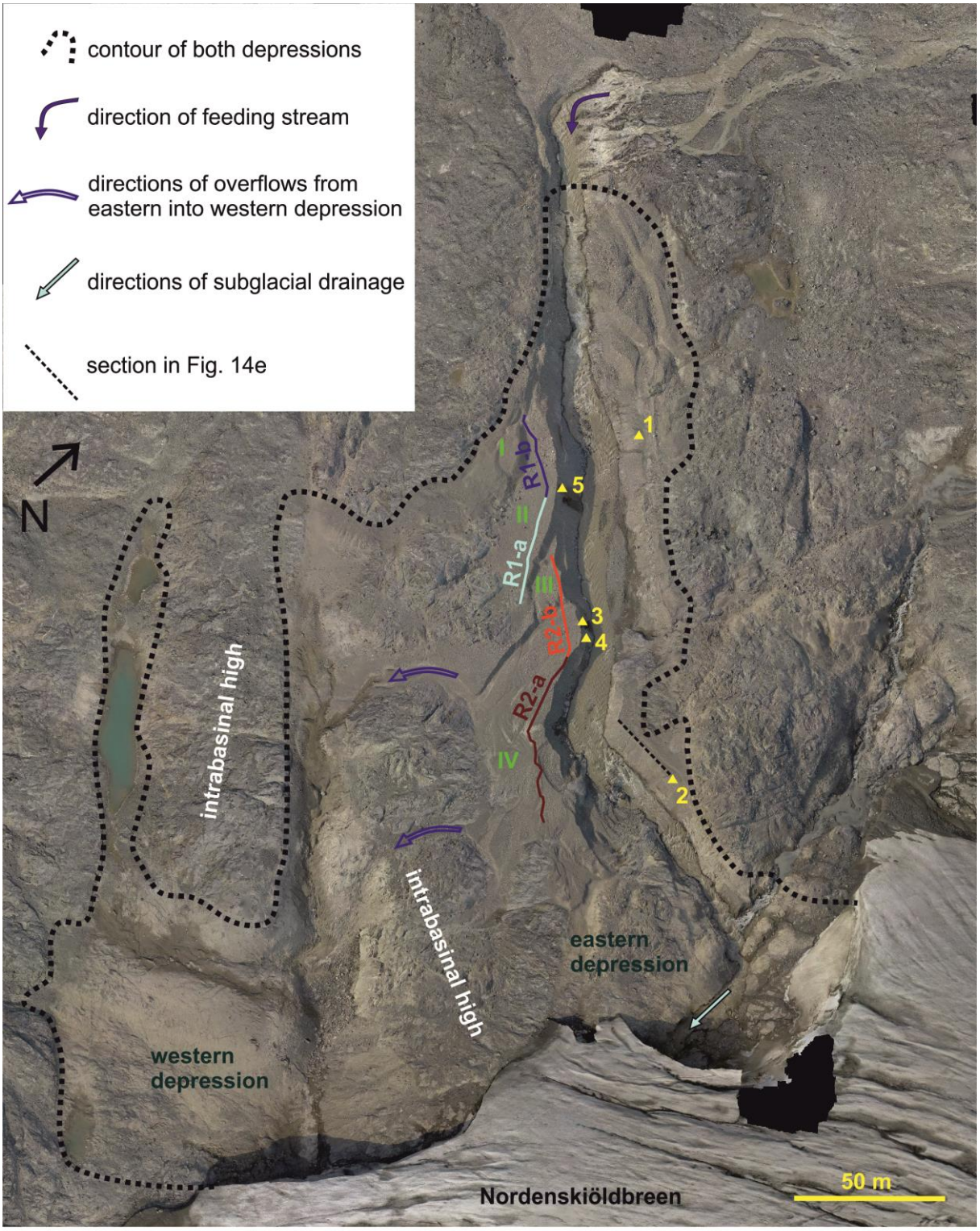

Fig. 2

ACCEPTED MANUSCRIPT

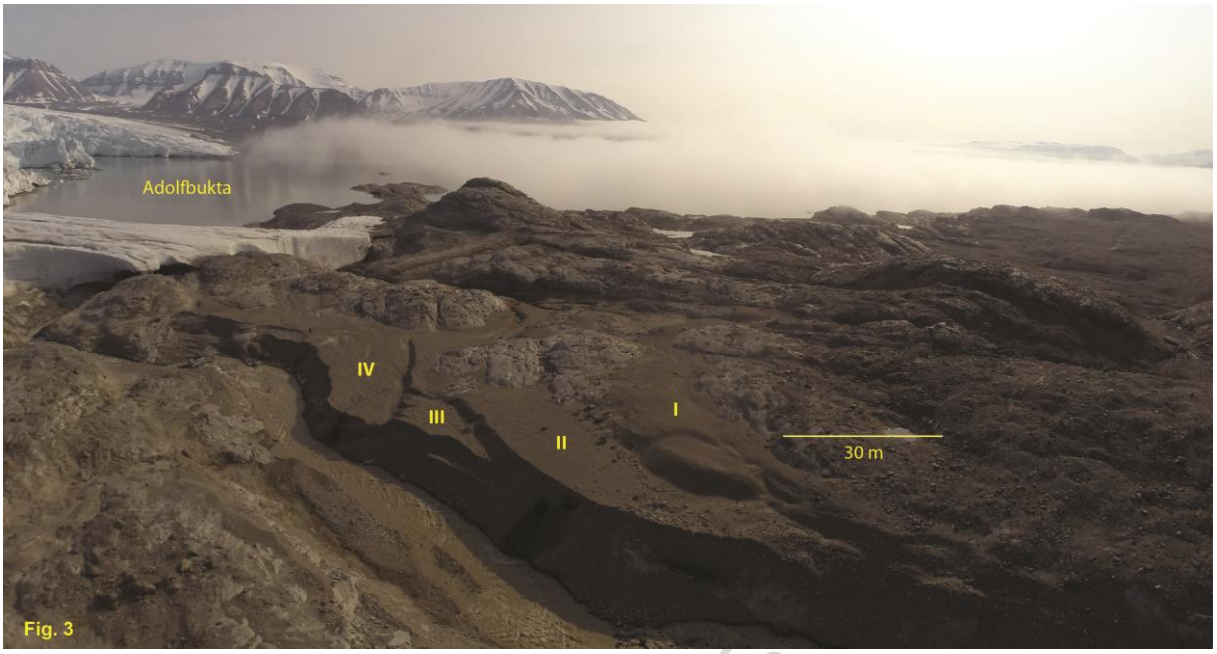

Fig. 3

ACCEPTED MANUSCRIPT

ACCEPTED MANUSCRIPT

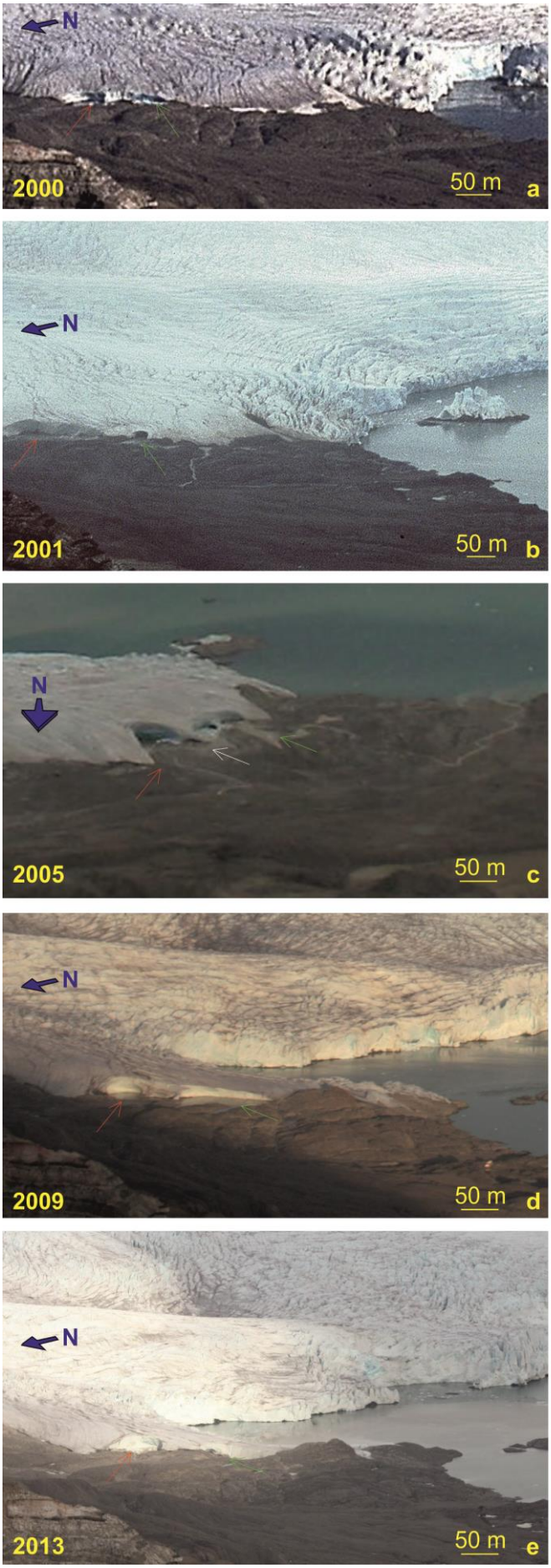

Fig. 4

ACCEPTED MANUSCRIPT

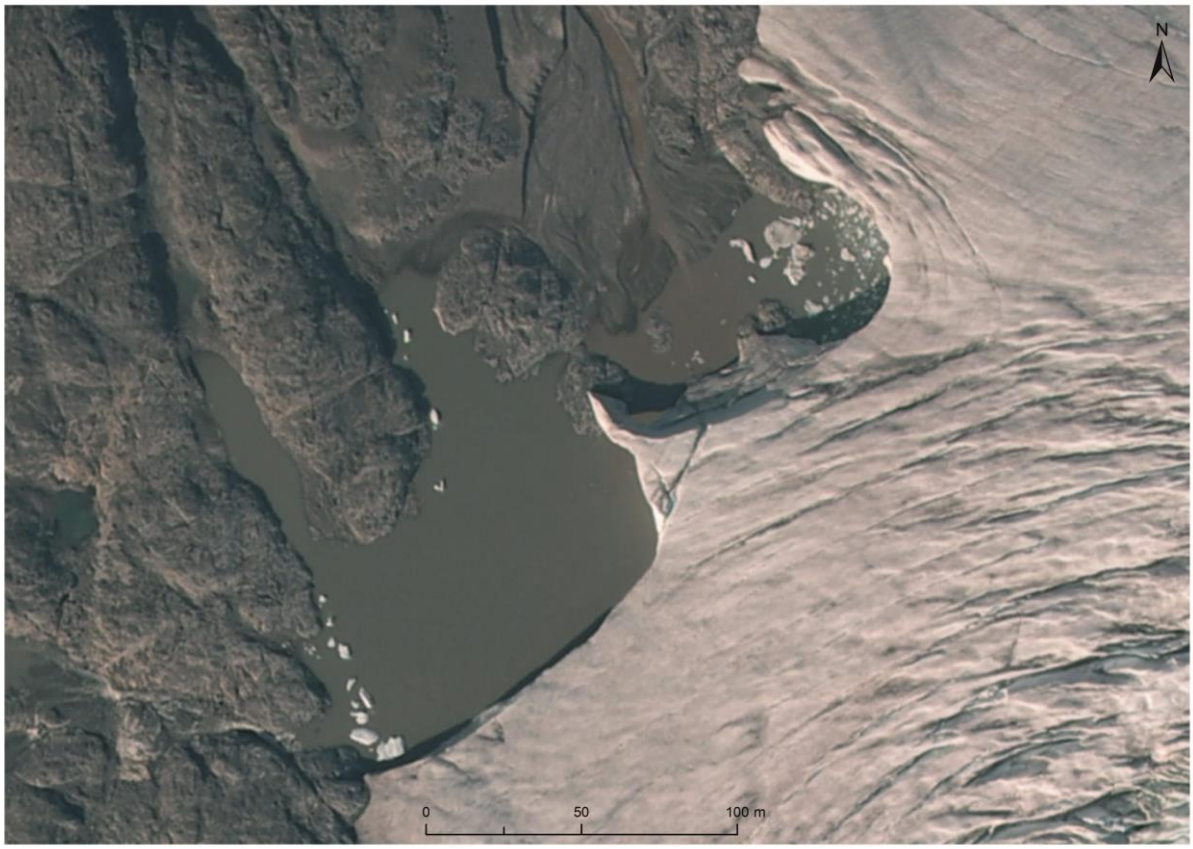

Fig. 5

ACCEPTED

ACCEPTED MANUSCRIPT

Fig. 6

ACCEPTED MANUSCRIPT

ACCEPTED MANUSCRIPT

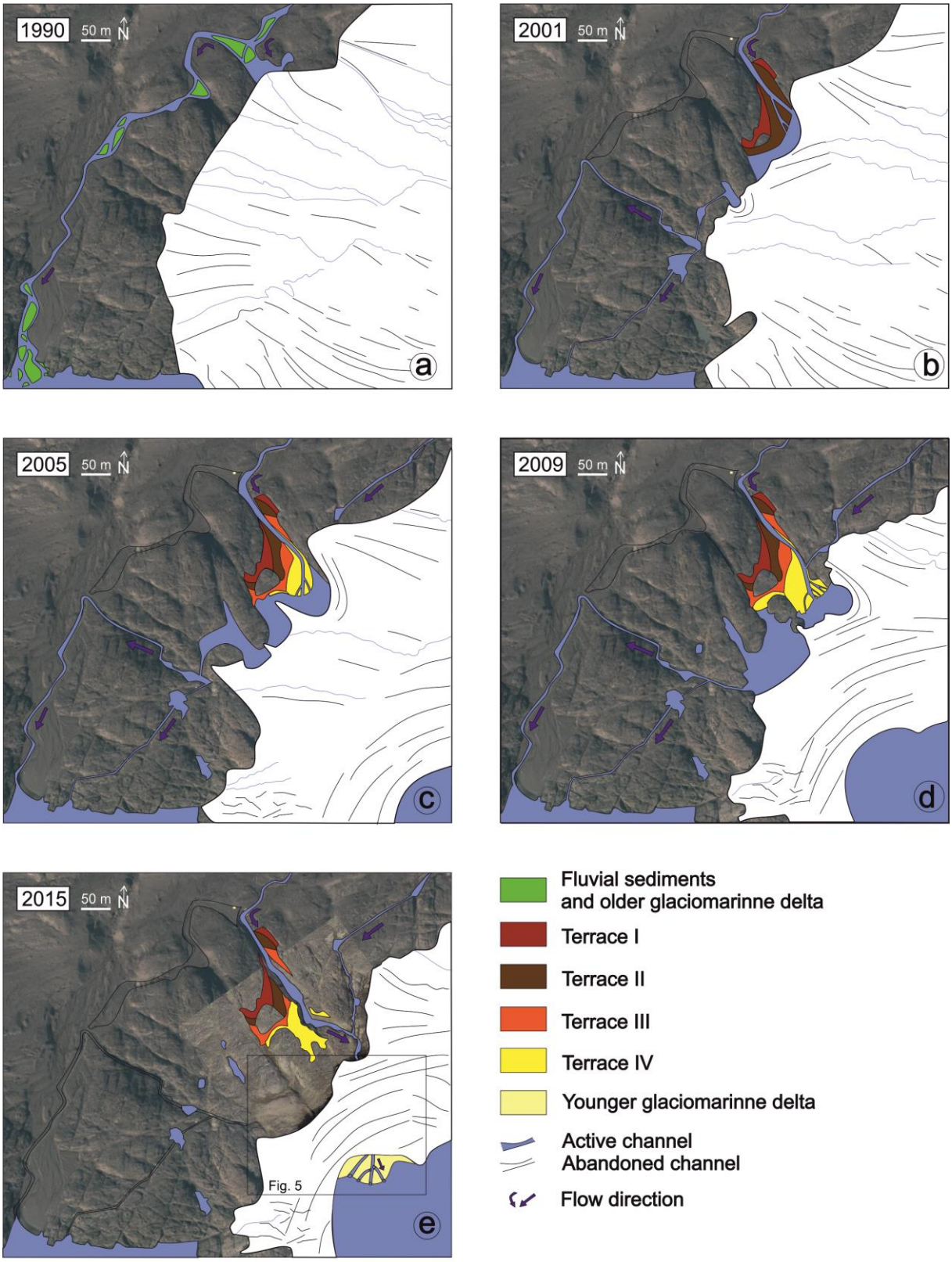

Fig. 7

ACCEPTED MANUSCRIPT

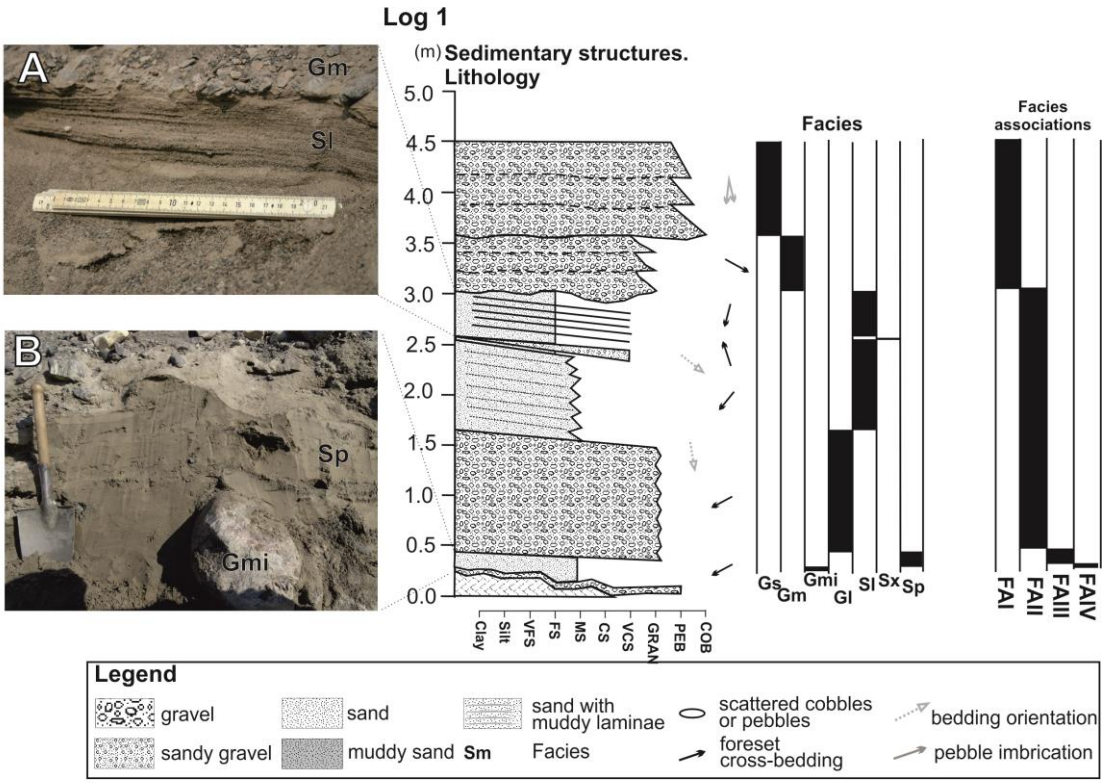

Fig. 8

ACCEPTED MANUSCRIPT

ACCEPTED MANUSCRIPT

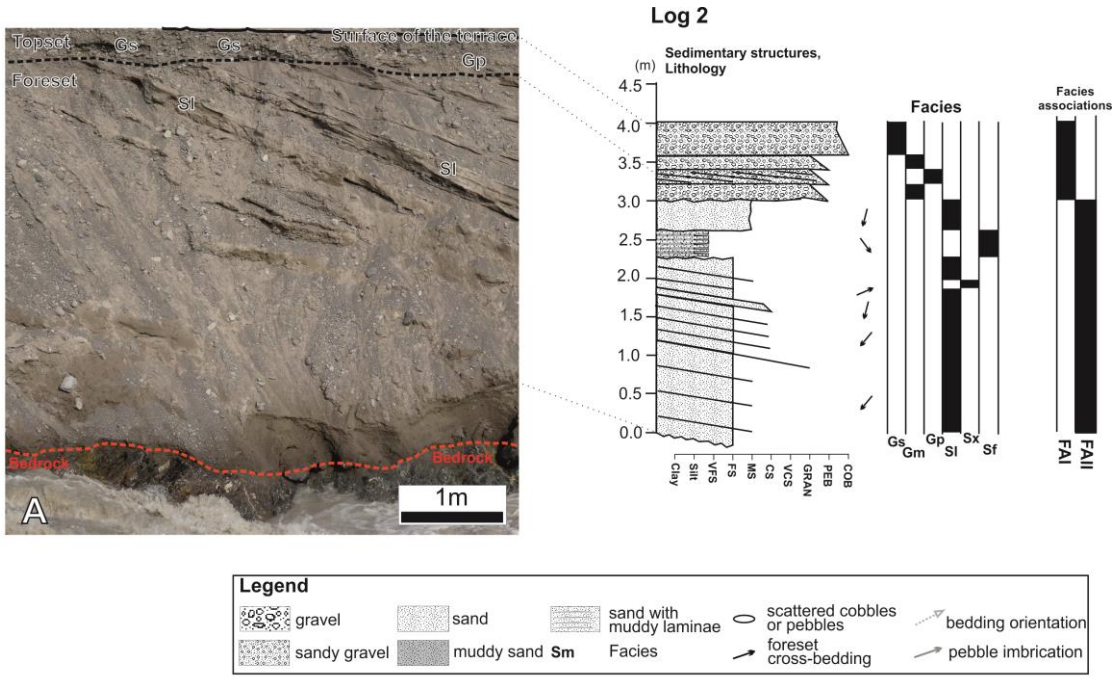

Fig. 9

ACCEPTED MA

ACCEPTED MANUSCRIPT

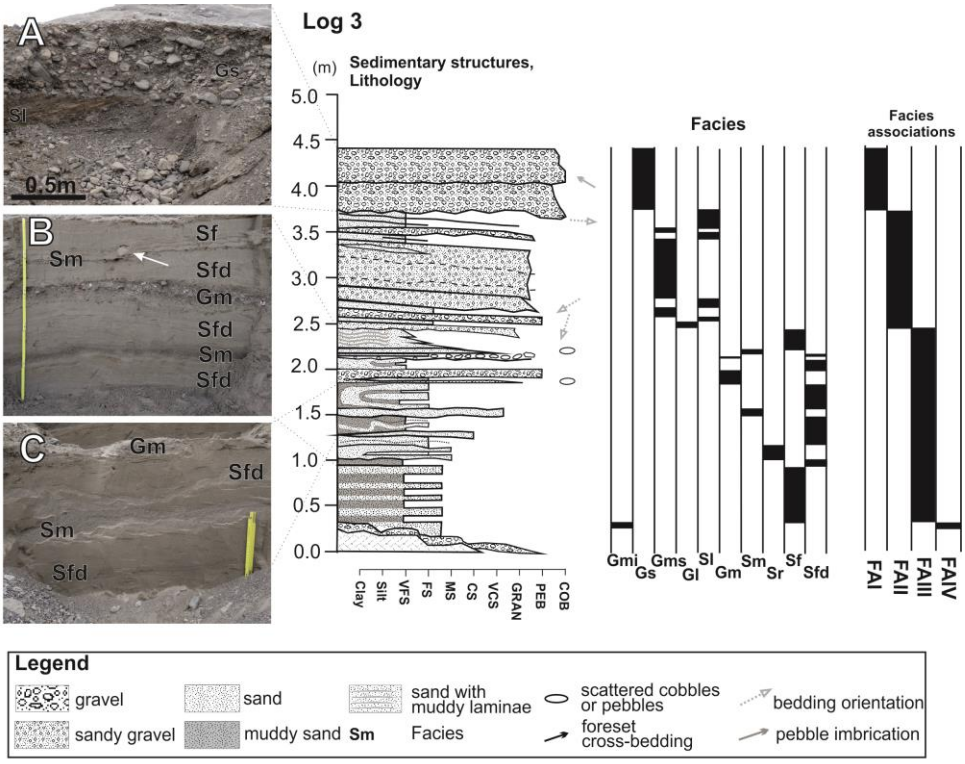

Fig.10

ACCEPTED MA

ACCEPTED MANUSCRIPT

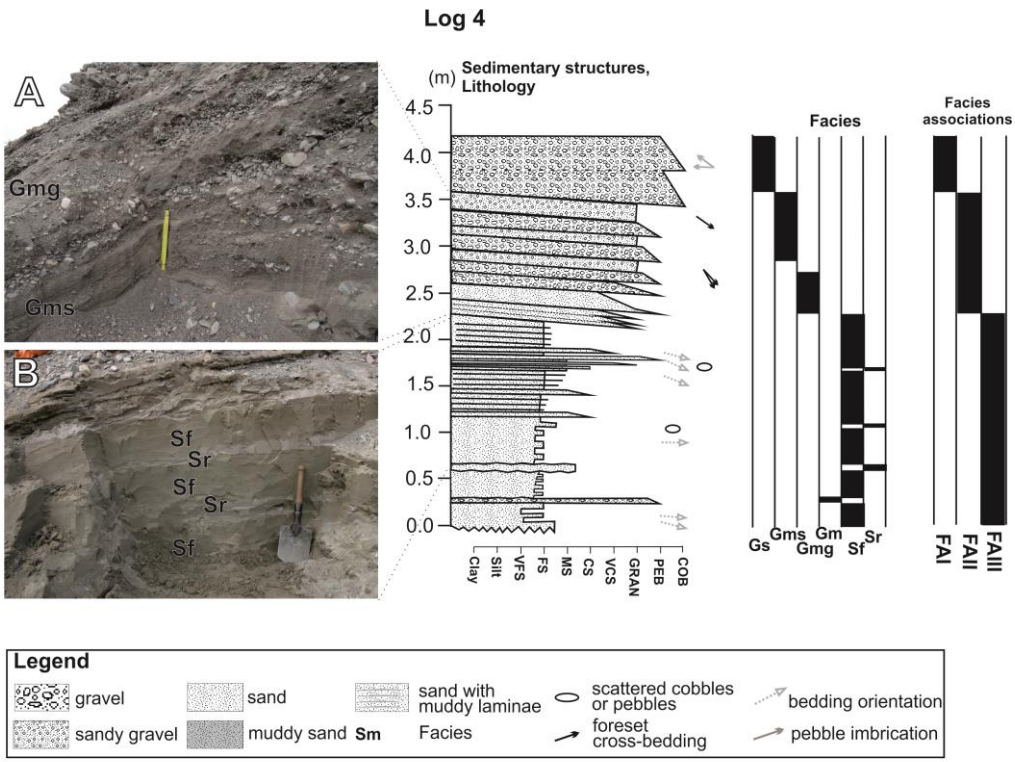

Fig. 11

ACCEPTED MANUSCRIPT

ACCEPTED MANUSCRIPT

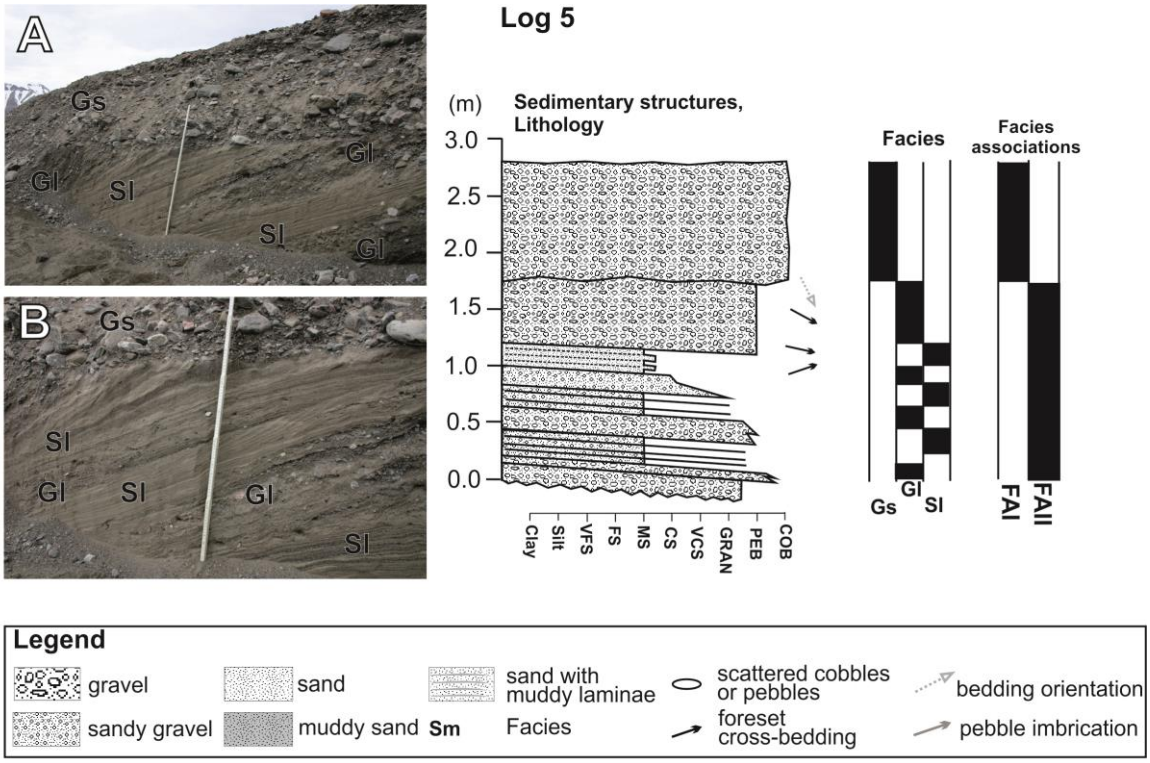

Fig. 12

ACCEPTED MANUSCRIPT

ACCEPTED MANUSCRIPT

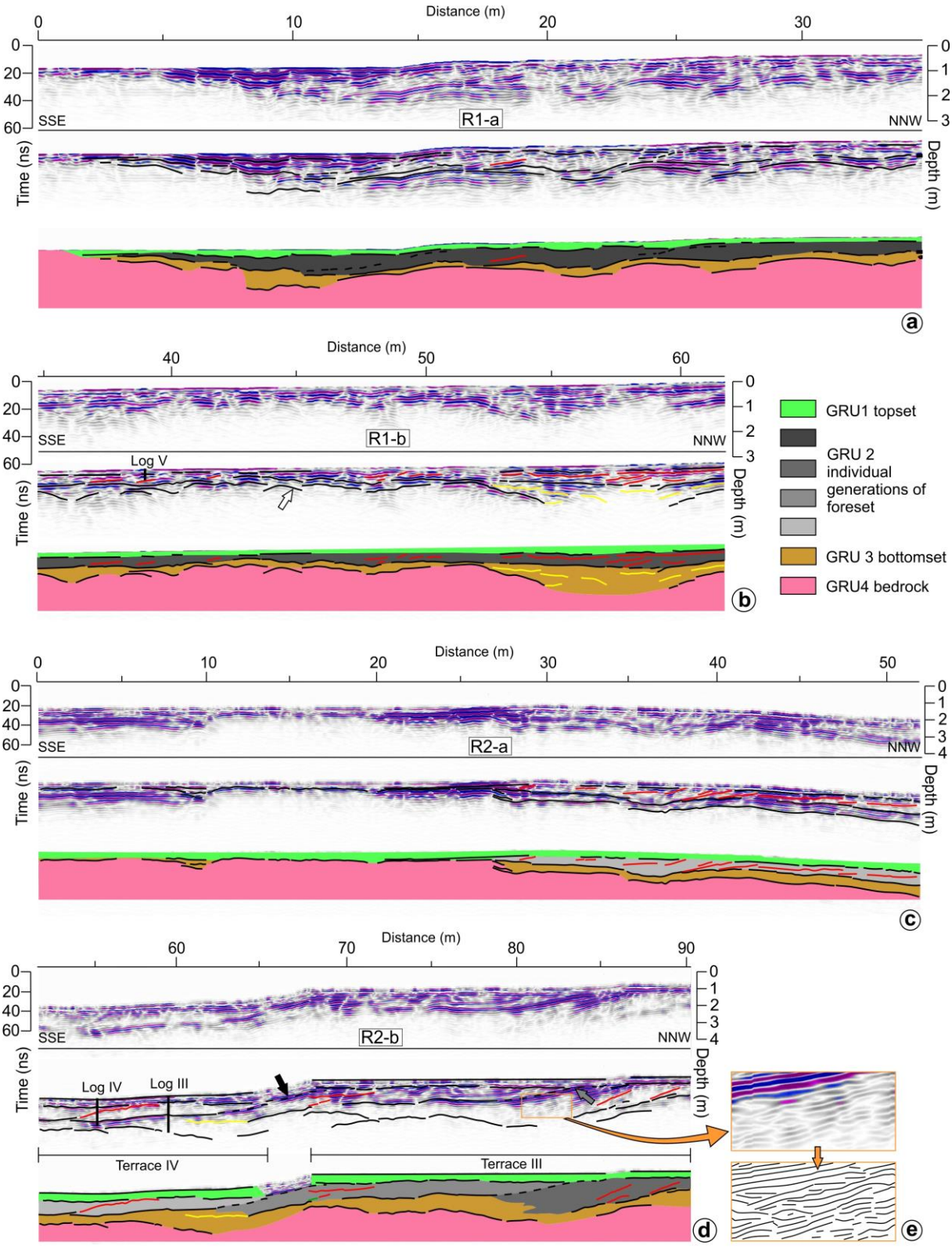

Fig. 13

ACCEPTED MANUSCRIPT

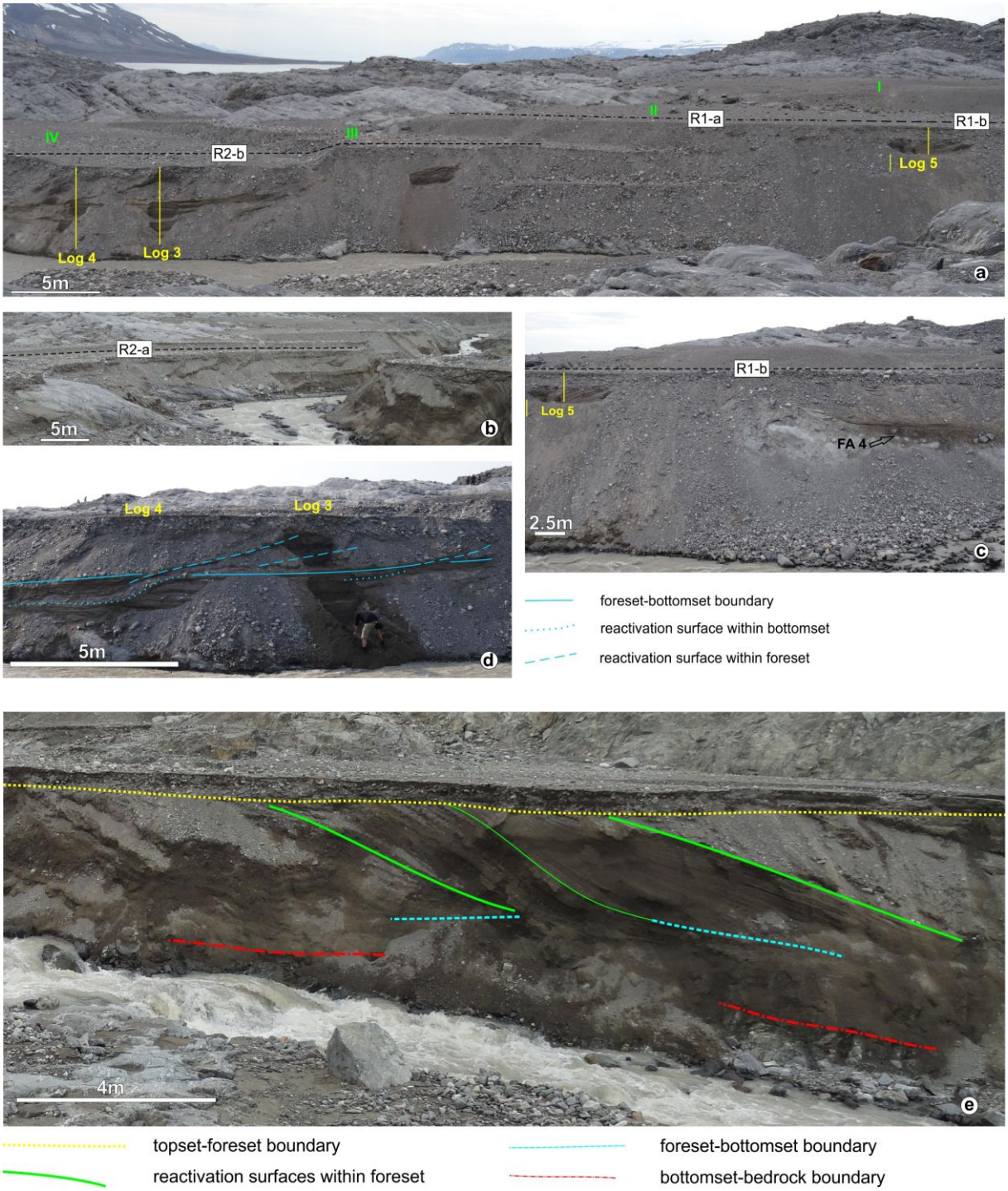

Fig. 14

ACCEPTED MANUSCRIPT

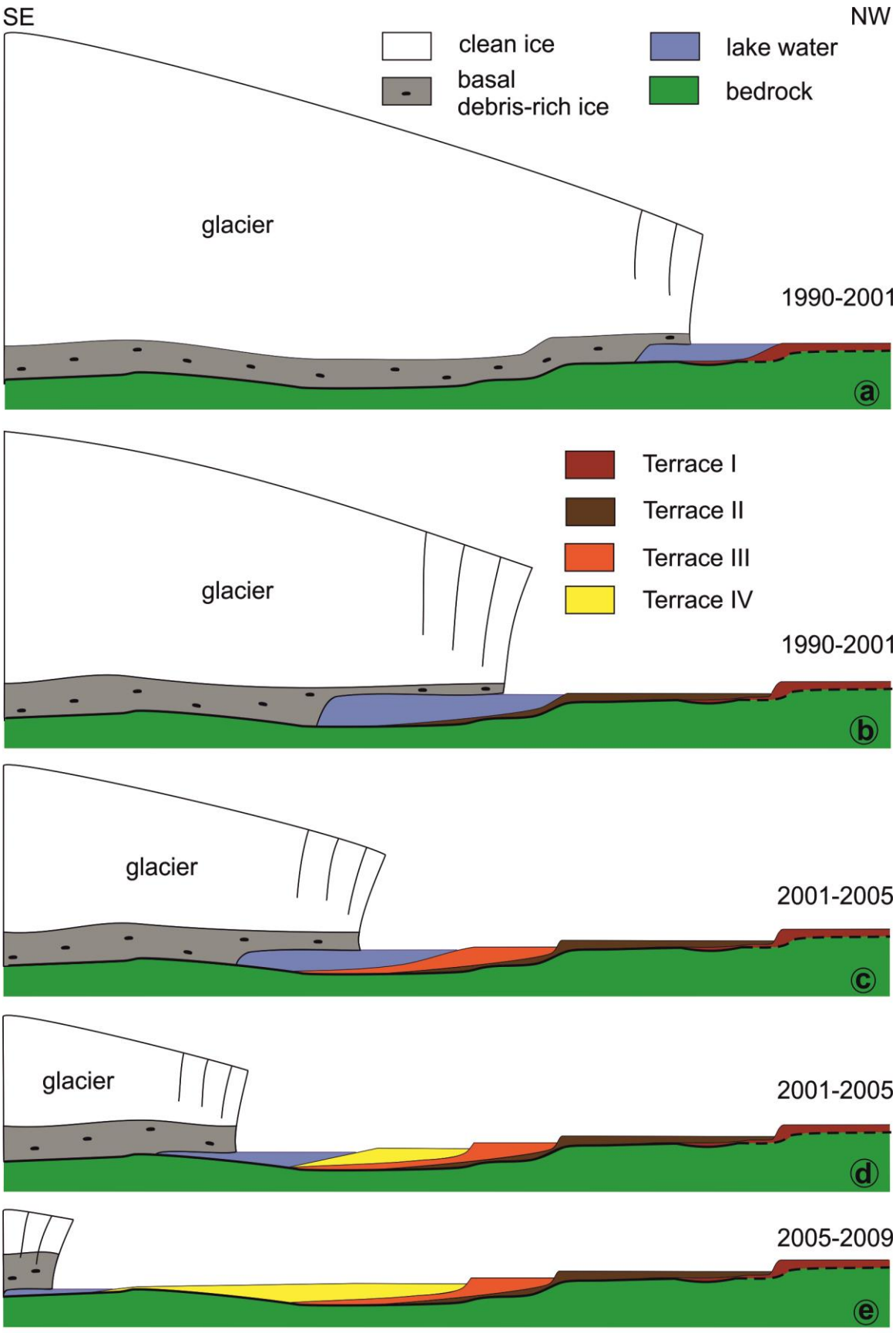

Fig. 15

ACCEPTED MANUSCRIPT

Table 1:

Subhorizontal coarse grained beds		
Symbol	Description	Interpretation
Gs	Clast-supported pebble to cobble gravel with horizons of openwork texture. Massive to crude planar stratification. Subrounded to well-rounded clasts mostly up to 10 cm in diameter with both a 'rolling' a(t) b(i) and also a(p) a(i) fabric. Individual subborizontal sets are 7 to 15cm thick, coset thickness of 0.6-1.1 m. Tabular to wedge shape beds. Erosive inclined base. The coarsest clasts (rare boulders A max. 45 cm) irregularly scattered along the base. Flat or convex up top.	Tractional deposition of gravel as longitudinal bars ('sheet bars') in braided-stream channels (Boothroyd & Ashley, 1975; Nemec & Postma, 1993).
Gm	Matrix to clast-supported, massive pebbly sand or sandy gravel. Horizontal to gently inclined (≤10°) beds, tabular to lenticular shape of beds. Fining-upward sets (set thickness of about 10 cm) stacked in cosets up to 65 cm thick. Erosive slightly undulated base. The coarsest clasts (pebbles up to 5 cm) irregularly scattered along the base.	Tractional deposition of bedload gravel as pavement and sheet bars in braided-stream channels (Nemec & Postma, 1993; Miall, 1996).
Gp	Matrix to clast-supported, cross-stratified pebbly sand or sandy gravel. Isolated beds within facies Gm. Bed thickness 10-20cm. Horizontal to gently inclined (≤10°) beds. Erosive slightly undulated base. The coarsest clasts (pebbles up to 5 cm) irregularly scattered along the base.	Fluvial bedload, migration of small 2 D dunes (Miall 1996).
Gmi	Matrix supported massive pebble gravel, poorly sorted, subrounded to rounded pebbles and cobbles up to 16 cm. Matrix is formed by gravelly sand. Irregular shape of beds, beds are discontinuous. Max. thickness mostly only several centimetres, rarely up 16 cm thick.	Partly reworked coarse grained clasts from basal debris-rich ice (Allaart, 2016).
High-angle inclined beds		
Gl	Planar parallel–stratified very coarse sand, pebbly sand or sandy gravel, frequent grain-size fluctuations on a thickness scale of a few cm. Subrounded to rounded pebbles up to 6 cm. Elongated pebbles oriented commonly parallel to subparallel with stratification. Inclined tabular beds, thickness of about 120 cm. Inclination between 20^{o} and 30^{o}.	Tractional deposition by high-density turbidity current (Talling et al. 2012), hyperpycnal flow of Lowe (1982).
Sl	Planar parallel–stratified fine, medium to fine, medium	High-density turbidity

ACCEPTED MANUSCRIPT

	to coarse grained sand with subordinate laminas of very coarse sand or strings of pebble gravels (A max 5 cm). Frequent grain-size fluctuations on a thickness scale of 3 to 5 cm. Inclined tabular to wedge shaped beds, thickness up to 220 cm, set thickness about 10-30 cm. Inclination between 20^{o} and 30^{o}.	current (Talling et al. 2012)
Sx	Solitary backsets of very coarse sand cross-strata dipping upslope at ca 110-170° relative to the foreset bedding, filling trough-shaped scours about 15 cm deep oriented only slightly oblique (about 40^{o}) to foresets.	Slope chute-fills (Nemec, 1990), deposits of chute-and-pools or cyclic steps (Lang & Winsemann 2013).
Gmg	Massive, normally (distribution grading) graded pebbly sand, granule gravel or pebble gravel, sets 5 to 18 cm thick, passing upward into faintly planar parallel-stratified sand, sets 10- 12 cm thick, flat base. Pebbles along the base up to 4 cm in diameter. Inclination of beds about 20^{o} -22^{o}.	Deposition by high-density turbidity currents (sensu Lowe, 1982)(Gobo et al. 2014 a, b). Surge-type flows.
Gms	Clast-supported massive pebble gravels, locally openwork, solitary set 5 to 15 cm thick or coset up to 65 cm thick. Almost flat, slightly undulated non-erosional bases, flat tops. Rare cobbles up to 8 cm, mostly rounded to subrounded pebbles and granules. Granules and very coarse sand represent matrix. Tabular to wedge shape of beds. No preferred orientation of elongate clasts. Inclination of beds about 20^{o} -22^{o}.	Cohesionless debris flows.Openwork indicate that the deposition occurs near the subglacial conduit exit (Russell & Arnott, 2003; Hornung et al., 2007)
Low-angle inclined fine-grained beds		
Sf	Rhythmic alternation of laminas to thin beds (up to 5 cm) of silty sand or very fine sand and laminas of fine to medium or medium to coarse grained sand. Planar parallel lamination, horizontal or low-angle inclined (max. 5^{o}) planar lamination or undulated lamination. Well sorted. Wedge to tabular shape of beds. Max. recognised thickness of 40 cm, commonly thickness to 10 cm. Generally flat base, irregular erosive top of beds. Exceptional isolated pebbles about 5 cm in diameter especially along the base.	Alternating deposition from suspension and hyperpycnal underflows (low-density turbidity currents - Lowe 1982). Isolated pebbles are interpreted as dropstones (Ravier et al. 2014).
Sfd	Irregular alternation of laminas to thin beds (up to 5 cm) of silty sand or very fine sand and laminas of fine to medium or medium to coarse grained sand. Deformed – convolute lamination, undulated, contorted, irregular top and base. Irregular shape of the beds. Max. recognised thickness of 30 cm.	Syn-sedimentary and early post-sedimentary deformed beds of facies Sf (Pisarska-Jamrozy, Weckerth 2013).

ACCEPTED MANUSCRIPT

Sr	Medium, medium to coarse grained well sorted sand, trough cross-ripple lamination, (3D ripples). Irregular slightly undulated base, convex up top. Coset thickness of about 15 cm.	Depositio from low-energy tractional flows (Mulder & Alexander, 2001).
Sm	Coarse to very coarse sand, massive, beds up to 7 cm thick, sharp slightly undulated base, irregular slightly convex up top. Thickness of beds of about 7 cm.	Fine-grained suspension deposits (Eilertsen et al. 2011)

ACCEPTED MANUSCRIPT